Colloids and Surfaces A: Physicochemical and Engineering Aspects 749 (2026) 141166

Contents lists available at ScienceDirect

Colloids and Surfaces A: Physicochemical and Engineering Aspects

journal homepage: www.elsevier.com/locate/colsurfa

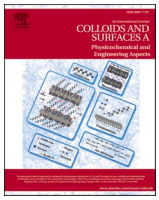

Effect of cyclic molecules on salt curves of mixed anionic-zwitterionic surfactant solutions

Z. Mitrinova [a], N. Pagureva [a], N. Burdzhiev [b], S. Tcholakova [a,c,*]

[a] Department of Chemical and Pharmaceutical Engineering, Faculty of Chemistry and Pharmacy, Sofia University, 1 J. Bourchier Ave., Sofia 1164, Bulgaria
[b] Department of Organic Chemistry and Pharmacognosy, Faculty of Chemistry and Pharmacy, Sofia University, Sofia 1164, Bulgaria
[c] Centre of Competence "Sustainable Utilization of Bio-resources and Waste of Medicinal and Aromatic Plants for Innovative Bioactive Products" (BIORESOURCES BG), Sofia, Bulgaria

GRAPHICAL ABSTRACT

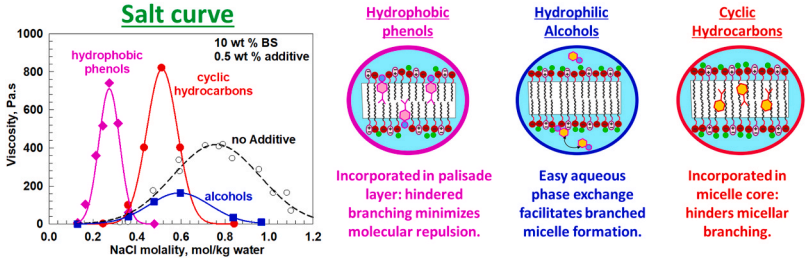

ARTICLE INFO

Keywords:
Wormlike micelles
Salt curves
Perfumes
Ionic strength
Rheology
Octanol-water partitioning coefficient
Molecular volume

ABSTRACT

The effect of twelve cyclic molecules on the rheological response of a 10 wt% mixture of sodium lauryl ether sulfate and cocoamidopropyl betaine (BS) was evaluated. The results demonstrate that all studied additives effectively reduced the salt concentration required to reach peak viscosity and narrowed the width of the salt curve. The specific effect on the magnitude of the peak viscosity depends on the molecular structure of the additive. Hydrocarbons, along with hydrophobic phenols, increase the peak viscosity, while alcohols and simple phenol, decrease it. SAXS and NMR measurements revealed that hydrocarbons are primarily incorporated into the micellar core, and the observed viscosity enhancement is attributed to the suppression of micellar branching. In contrast, molecules possessing an OH-group intercalate between the surfactant headgroups or reside at the micellar surface. For hydrophobic phenols, the ability to form stable hydrogen bonds results in a significant increase in the maximum viscosity. This interaction substantially reduces the salt concentration required to reach peak viscosity; in this case, the micellar charge density remains relatively high, and electrostatic repulsion hinders micellar branching. On the other hand, simple phenols and alcohols decrease viscosity because their higher water solubility allows them to easily redistribute across different regions of the micelle surface, thereby facilitating micellar branching. The dimensionless parameters accounting for the effect of the studied additives on the salt curve characteristics were determined. These parameters were shown to depend on a composite molecular parameter, defined as the ratio of the surfactant volume to the additive volume multiplied by the octanol–water partition coefficient, $v_{BS}/v_A LogP$.

* Corresponding author at: Department of Chemical and Pharmaceutical Engineering, Faculty of Chemistry and Pharmacy, Sofia University, 1 James Bourchier Ave., Sofia 1164, Bulgaria.
E-mail address: SC@LCPE.UNI-SOFIA.BG (S. Tcholakova).

https://doi.org/10.1016/j.colsurfa.2026.141166
Received 4 May 2026; Received in revised form 14 June 2026; Accepted 24 June 2026
Available online 25 June 2026

1. Introduction

Micellar solutions are used as cosmetic and house care products. Typically, ionic micelles are affected by the presence of electrolyte which change their rheological response and phase behavior [1–11].

In addition, the micelles are able to solubilize different type of molecules including hydrophobic one (weakly soluble in the aqueous phase). Molecules with moderate hydrophobicity induces micellar elongation [5,6,12–20]. There is an optimal chain length of linear fatty alcohols which leads to the highest viscosity of anionic + zwitterionic surfactant mixture [12]. The molecule architecture is also important and the presence of branches and double bonds in the hydrocarbon backbone decreases the effect of co-surfactant on micellar growth because of the additional freedom of the molecules to rotate along the double bond which hinders close packing of the tails [8].

Generally, more hydrophilic co-surfactants are located predominantly in micelles palisade layer, while more hydrophobic in the hydrocarbon core [15–17]. And the molecule positioning governs the micellar size in a such a way that the additives with intermediate *LogP* have the highest contribution to the micellar growth [18].

The solubilized molecules affect not only the micelles per se but also the salt curve of the surfactant solutions or the micellar transformations upon addition of salt. McCoy et al., showed that cyclic molecules transform zwitterionic worm-like micelles (WLM) into microemulsion unless resonance structure between benzene ring and hydroxyl groups are formed [19]. The latter case leads to viscosity increase, which is related to additional screening of surfactant charges due to proton donation.

Parker et al., showed that fragrance molecules shift the viscosity peak of anionic sodium lauryl ether sulfate (SLES) salt curves leftward [5]. The authors determine amphiphilic co-surfactants which are localized near to the micellar interface and shift the viscosity maximum position to the lower salt concentrations [5] while long chained hydrocarbons have opposite effect and lead to demixing expressed as rightward shift [6]. The effect on the maximal viscosity could be negative for more hydrophilic molecules which lower the micellar bending constant resulting in persistence length and viscosity decrease [5] or positive for cyclic hydrocarbons acting like interface stiffener [6].

The increase in molecule hydrophobicity at similar charge sodium methyl salicylate instead of sodium salicylate enhances micellar core shielding which leads to anisotropic micellar growth. Thus, resulting in less additive required to induce changes in the viscoelastic properties and leads to higher viscosity maximum in presence of salt [20]. Comparison between sodium salicylate and salicylic acid showed that charged additives stay trapped at the polar shell, and that acid forms are less efficient for charge neutralization [21]. The authors conclude that, the most efficient for micellar growth are partially hydrophobic molecules due to the core densification and shielding from water accompanied by screening of the electrostatic repulsion between head groups. Thus, the concept for intermediate hydrophobicity is operative for the effect on viscosity in presence of studied additives.

The effect of molecules polarity on the solubilization and localization in surfactant micelles have been previously studied for surfactant systems. It is known that molecules with intermediate polarity or *LogP* increase in the highest extent the micellar size [16,17] and thus solution viscosity [18]. At high $LogP > 3.5$ molecules are fully solubilized in the sodium dodecyl sulfate (SDS) micelles and locate near the micellar core, causing significant micelle swelling, while at low $LogP < 2$ they are partially incorporated into the SDS micelles and locate in the headgroup regions, so they almost do not change the size of the micelles [16]. For moderately hydrophobic molecules the size and aggregation number of SDS/perfume micelles is the biggest [16]. It is noted that the fluctuations in the results could be attributed to the influence of other molecular structure factors besides the degree of hydrophilicity/hydrophobicity, like perfume–perfume interactions and the surfactant tail structure [22]. Recently was shown that the highest effect on solution viscosity is observed with resonance structures of aromatic compound containing oxygen atoms [19].

Other study showed that the perfume molecules incorporation in Pluronic micelle is enhanced for the systems with the lowest oil-water interfacial tensions [23]. The authors claim that the molecule positioning is determined by the interplay between polarity, water solubility, water-oil interfacial tension and molecular architecture. Study of polymer Soluplus or PEG-g-(PVAc-co-PVCL) also showed that the prediction of system properties could not be reliable only on *LogP* but one should also consider the presence of specific functional groups and the molecular conformation [24].

Recently, we analyzed the effect of linear molecules octanol and octyl trimethyl ammonium bromide on SLES + CAPB (cocoamidopropyl betaine) salt curves [25]. Both nonionic and cationic co-surfactant with similar chain length significantly shift the surfactant salt curves leftward which means that they facilitate WLM formation. Octanol molecules incorporate between main surfactant and decrease mean area per molecule, which results in a higher packing parameter which decreases the fraction of ionized species (SLES anions) that should be neutralized by the counterions in order to increase packing parameter ensuring WLM formation. On the other hand, C8TAB neutralizes some of the SLES anions without affecting the area per molecule.

The effect of single molecules of different types (aliphatic, aromatic, cyclic) on surfactant micelles are well established. For example, essential oils or their components in polymeric solutions [23,26,27], zwitterionic [19,28] or anionic + zwitterionic micellar solutions [22,29,30] are analyzed via SAXS, SANS and NMR. In such formulations, surfactant aggregates serve as carrier systems of predominantly hydrophobic fragrance molecules. However, the area could be further broadened in order to investigate the effect of molecular structure on the salt curves of mixed surfactant systems for a broader range of molecules with varying parameters.

As demonstrated by this overview, previous literature can be divided into two categories: (1) studies that evaluate the effect of additive molecules at a fixed electrolyte concentration [12,15–18,22] from which it remains unclear how the additives affect the salt curve characteristics (maximal viscosity, the salt concentration required to reach maximal viscosity and the width of the salt curve). and (2) studies that measure full salt curves in presence of a given additive concentration, but do so exclusively within single-surfactant systems such as SLES [5,6,13], CTAB [19,21], or betaine [20]. This leaves a knowledge gap regarding how additive molecules modulate the cooperative packing and viscoelastic profile of the mixed surfactant systems.

The major aim of the current study is to determine the effect 12 different cyclic molecules on the rheological properties of industrially relevant sodium dodecyl ether sulfate (SLES) and cocoamidopropyl betaine (CAPB) mixture, typical of commercial shampoo formulations, at different salt and additive concentrations. The second aim is to establish the relationship between the molecular characteristics of the additive molecules and their impact on the salt curve characteristics.

To achive these aims, we first determine the effect of additive concentration on the rheological properties of BS system in the absence of salt, and subsequently evaluate how a fixed additive concentration shifts the salt curve. For a subset of these additives, the salt curve characteristics are additionally determined at two different additive concentrations. Finally, we establish a correlation between salt curve characteristics and the molecular characteristics of the additives.

2. Materials and methods

2.1. Materials

The surfactant system, denoted as BS in the text, is a mixture of sodium lauryl ether sulfate, SLES (product of Stepan Co., IL, USA; with commercial name STEOL CS−170 Stepan) and cocoamidopropyl betaine, CAPB (product of Goldschmith, with commercial name Tego

Betaine F50). Twelve different cyclic molecules are studied as co-surfactants, see Table S1: (1) three aromatic hydrocarbons: 1,4-Di-iso-propylbenzene (denoted as DIPB), p-cymene (pCMN), toluene (TLN); (2) two alicyclic hydrocarbons: γ-Terpinene (GTPN) and Limonene (LMN); (3) three phenols: simple phenol (PhOH), and two hydrophobic phenols: thymol (ThOH) and carvacrol (CarOH); (4) One aromatic alcohol – benzyl alcohol (BOH) and (5) Three alicyclic alcohols: L-mentol (MOH), (+)-terpinen−4-ol (TerOH) and cyclohexanol (CycOH). Seven of them have hydroxylic group in their structures (PhOH, ThOH, CarOH, BOH, MOH, TerOH and CycOH) and five of them do not have polar part (DIPB, pCMN, TLN, GTPN, LMN). Aromatic hydrocarbons, phenols and aromatic alcohols have planar part in their structure because they possess benzene ring, whereas the alicyclic hydrocarbons and alicyclic alcohols do not have planar part.

Note that most of the studied additives are the primary constituents of well-known essential oils. Specifically, LMN is the major component of lemon and orange oils, whereas TerOH and GTPN serve as the main components in tea tree oil. ThOH and CarOH represent the primary constituents of oregano oil, whereas pCMN is commonly found in tea tree, lemon, and orange oils. Additionally, MOH is principal component of peppermint oil, and BOH is a characteristic volatile constituent found in rose oil.

Samples were prepared from 15 wt% SLES + CAPB (2:1) stock solution in deionized water, purified by Milli-Q Organex system (Millipore Inc., USA). The surfactant mixture was homogenized by stirring at room temperature until full dissolution of the components. Initial electrolyte solution was prepared at 2 M concentration. The working samples were prepared by consecutively mixing co-surfactants, stock surfactant solution, de-ionized water and finally concentrated salt solution. In all cases mild stirring was applied until homogeneous solution were obtained (at least 1 h). All samples were prepared at room temperature except for ThOH which was heated to 50 °C corresponding to its melting point.

Most of the studied samples contained 10 wt% (≈300 mM) main surfactants mixture, 0.5 wt% component and electrolyte concentration varied in the range 0–0.6 M. In order to determine the solubility limit of the compounds in BS system their concentration was varied in the range between 0.25 and 33 wt% in absence of any added salt. For building the salt curves sodium chloride (NaCl) product of Sigma Aldrich was added in the mixtures.

It should be noted that the zwitterionic CAPB surfactant contains NaCl, which was found to be 112 mM NaCl for a 100 mM CAPB solution [31]. Because the total surfactant concentration in all studied systems is kept constant at 200 mM SLES and 100 mM CAPB, this background NaCl concentration remains fixed at 112 mM, even prior to any intentional salt addition. Consequently, for all salt curves presented in this manuscript, the total NaCl concentration is calculated as the sum of the NaCl originating from CAPB and the additionally introduced NaCl.

All prepared samples were kept at room temperature and the analysis were performed at least one day after their preparation. Mixtures were transparent (except when other is specified) and homogeneous without indication of phase separation for at least one year after their preparation.

2.2. Rheological properties

Rheological measurements were performed on rotational rheometer Bohlin Gemini (Malvern Instruments, UK). Measurements were performed by using cone and plate geometry with two different cone diameters depending on solution viscosity. For low viscous samples $\eta < 1$ Pa·s, a geometry with 60 mm cone diameter and 2° truncation was used, and for those with viscosity above 1 Pa·s, plate with 40 mm cone and 4° truncational angle.

The protocol for rheological measurements consists of 5 min thermal equilibration and consecutive logarithmical variation of shear rate in the range of 0.01 s^{-1} and 300 s^{-1}. The viscosity of each sample was measured by 2 independent measurements and the error was determined to be around 10%. Oscillatory measurements were also performed at frequency sweep regime. The sample was equilibrated for 5 min at the working temperature and then frequency was varied between 0.01 and 10 Hz at 2% deformation, which correspond to the linear region in amplitude sweep experiment.

The rheological measurements were performed at least one day after sample preparation in order to equilibrate at room temperature and the measurement temperature was set to 20 °C.

2.3. Optical microscopy

The optical observations of the samples above solubility limit of the additives in the BS system were provided on AxioImager (Zeiss, Germany) equipped with long-distance objective Zeiss epiplan 20x and 50x in transmitted polarized light. A few drops of the sample were placed on a microscope glass and cover glass was put above.

2.4. Nuclear magnetic resonance (NMR)

The NMR experiments are carried out on a Bruker Avance III HD 500 MHz spectrometer (Rheinstetten, Germany) fitted with a high-resolution broadband probe-head with Z gradient. Experiments are conducted at T = 25 °C. The studied samples are prepared as described in 2.1. 0.5 mL of the sample and 0.1 mL of deuterium oxide (99.8 atom % D) with TMSP-Na−2,2,3,3-d_4 as internal standard (0 ppm) are mixed before measurement. Topspin 3.6.5 software package (Bruker) is used for spectrum collection and data analysis.

2.5. Small angle X-ray scattering (SAXS)

SAXS measurements of the micellar solutions were carried out on an inhouse X-ray scattering system (XEUSS 3.0 SAXS/WAXS System, Xenocs, Sassenage, France) with a CuKα X-ray source (λ=0.154 nm, Xeuss 3.0 UHR Dual source Mo/Cu, Xenocs, Sassenage, France) and Eiger2 4 M detector (Dectris Ltd., Baden Deattwil, Switzerland) with slit collimation. The details for the experimental conditions are described in [7]. For the SAXS data modeling the software SASView was used.

3. Experimental results

3.1. Partitioning of cyclic molecules between water and BS micelles

Based on their maximal water solubility, we categorized the studied molecules into three groups, see Tables 1 and S1 (in Supporting information): (1) Group 1 includes molecules with very low water solubility (<1 mM): two aromatic hydrocarbons (DIPB and pCMN) and two alicyclic hydrocarbons (LMN and GTPN). These molecules have a molecular mass above 130 g/mol, do not possess OH group and their *LogP* values are above 4; (2) Group 2 includes molecules with intermediate water solubility (between 2 and 20 mM): one aromatic hydrocarbon (TLN), two hydrophobic phenols (ThOH and CarOH), and two alicyclic alcohols (MOH and TerOH). These molecules have *LogP* values between 2.6 and 3.5. The molecular mass in this group is split: molecules with an OH-group (ThOH, CarOH, MOH and TerOH) have a mass of approximately 150 g/mol, whereas Toluene, which does not have OH-group, has a mass of 92 g/mol; (3) Group 3 includes molecules with high water solubility (> 300 mM): one phenol (PhOH), one aromatic alcohol (BOH) and one alicyclic alcohol (CycOH). These molecules have a relatively low molecular mass of ≈ 100 g/mol and all of them have OH-group. Their *LogP* values are ≤ 1.5.

In the current study we determined the maximal solubility of these molecules in a 10 wt% BS solution (see Table S2). Group 1 (very low water solubility) have a relatively good solubility in the BS solution, ranging from 2.5 wt% (LMN) to 4.5 wt% (pCMN and GTPN). Group 3 (high water solubility) showed the highest overall solubility in 10 wt% BS solution, with maximal concentrations varying between 13 wt%

(BOH) and 29 wt% (PhOH). Group 2 (intermediate water solubility) exhibited the widest range of maximal solubility in 10 wt% BS. Hydrophobic phenols (CarOH and ThOH) were the least soluble in 10 wt% BS with limiting solubility of 1.3 wt%, whereas alicyclic alcohol (MOH) has intermediate solubility of 4 wt%, which is close to the solubility of molecules from Group 1. Toluene has a solubility of 6 wt% and other alicyclic alcohol (TerOH) showed the highest solubility in this group of 11.4 wt%, which is close to the solubility of molecules from Group 3 (high water solubility).

The determined limiting solubility in 10 wt% BS and the known solubility in water are used to calculate the partitioning coefficients of studied molecules between water, C_W and BS micelles, C_M. To determine the partitioning coefficient between the micellar phase and the aqueous solution, we assume that the maximum additive solubility measured in the 10 wt% BS solution is the cumulative sum of its intrinsic water solubility (obtained from literature and given in Table 1) and its maximum solubility within the micellar pseudophase. For instance, the maximum solubility of DIPB in a 10 wt% BS solution was determined to be 3.5 wt %. This corresponds to a clear formulation composed of 6.666 g SLES, 3.333 g CAPB, 0.615 g NaCl (inherent to the CAPB raw material), 3.5 g DIPB, and 85.886 g water. Within this system, only 2.14715×10^{-5} mol of DIPB is molecularly dissolved in the bulk water phase. Account for this aqueous fraction is necessary, as several of the studied additives exhibit significantly higher water solubilities. By difference, 0.02154 mol of DIPB is incorporated into the 10 g of BS surfactant micelles, indicating that 1 kg of BS surfactant can solubilize 2.154 mol of DIPB. Consequently, for DIPB, the micellar concentration is $C_M = 2.154$ mol/kg BS and the aqueous concentration is $C_W = 2.5 \times 10^{-4}$ mmol/kg water, yielding a partition coefficient of $Log[C_M/C_W] = 6.9$. Note that in this calculation the mass density of water and BS micelles is assumed to be equal to 1 g/mL.

The calculated values for partitioning of the studied molecules between aqueous solution and BS micelles are given in Table 1 and shown in Fig. 1 as a function of *LogP*, which shows the partitioning of these molecules between octanol/water. It is seen that the molecules from first group have $Log[C_M/C_W] > 4$ which agrees well with their *LogP* values. The only significant difference is observed for the most hydrophobic molecule investigated in the current study DIPB, which has higher value of $Log[C_M/C_W]$ as compared to *LogP* (6.9 vs 5.3) showing that this molecule is more soluble in the surfactant micelles as compared to octanol. There is also relatively good agreement between $Log[C_M/C_W]$ and *LogP* values for molecules from Group 3 (high water solubility), where the only significant difference is determined for cyclohexanol (1.8 vs 1.2) showing that this molecule also prefers to stay in BS micelles instead in octanol. The difference between $Log[C_M/C_W]$ and *LogP* is much more pronounced for hydrophobic phenols from second group namely CarOH and ThOH, for which $Log[C_M/C_W]$ is lower than *LogP* (2.0 vs 3.3) showing that these molecules are more soluble in octanol than in BS micelles.

Next, we studied the type of structures that are formed in the solutions when the concentration of the cyclic molecules exceeded their solubility limit in 10 wt% BS solution. Group 1 (low water solubility) and Group 3 (high water solubility) molecules formed liquid drops above their solubility limit concentration, whereas the molecules from

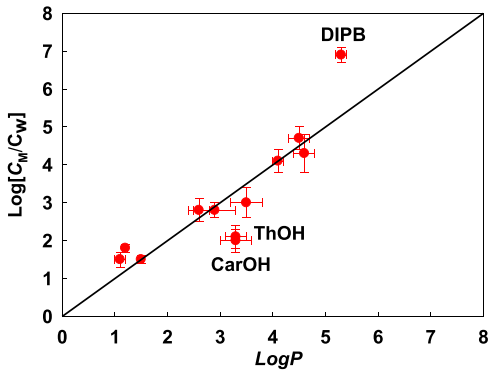

Fig. 1. Correlation between logarithm of partitioning coefficient between BS surfactant micelles and aqueous phase, $Log[C_M/C_W]$, and logarithm of partitioning coefficient between octanol and aqueous phase, *LogP*.

Table 1
Studied molecules, abbreviation used in the text, molecular mass, maximal solubility in water expressed in mmol/kg water, C_W, the distribution coefficient between octanol and water taken from the literature, *LogP*, the maximal solubility of additives in BS micelles expressed in mol per kg BS, C_M, logarithm of partitioning coefficient between micelles and water phases, $LogC_M/C_W$, core radius of micelles, R_C, formed in solution of 10 wt% BS + 0.5 wt% additive as determined from SAXS measurements and interfacial tension of water-dodecane containing 10 mol% additive and 5 mol% additive (data in paranthesis).

Molecule	Denoted in the text	M_A, g/mol	C_W, mmol/kg water	*Log P*	C_M, [mol/kg BS]	$LogC_M/C_W$	R_c,nm	IFT C12-water, mN/m
No additive	**-**	-	-	-	-	-	1.9	52.0
1,4-Di-iso-propylbenzene	**DIPB**	162.3	2.5×10^{-4} [32]	5.3 ± 0.1 [32,39]	2.2 ± 0.2	6.9 ± 0.2	2.2	33.4 (33.7)
γ-Terpinene	**GTPN**	136.2	0.064 [33]	4.5 ± 0.2 [33,40–43]	3.3 ± 0.4	4.7 ± 0.3	2.2	30.8
Limonene	**LMN**	136.2	0.1 [34]	4.6 ± 0.2 [44,45]	1.8 ± 0.4	4.3 ± 0.5	2.2	15.4 (16.5)
p-Cymene	**pCMN**	134.2	0.27 [35]	4.1 ± 0.1 [40,46,47]	3.4 ± 0.4	4.1 ± 0.3	2.1	39.4 (37.5)
L-menthol	**MOH**	156.3	2.75 [36]	3.5 ± 0.3 [40,48,49]	2.6 ± 0.4	3.0 ± 0.4	1.9	22.8
toluene	**TLN**	92.1	6.22 [19]	2.6 ± 0.2 [46,48,50–53]	3.8 ± 0.5	2.8 ± 0.3	2.0	47.4
Thymol	**ThOH**	150.2	6.55 [35]	3.3 ± 0.2 [48,54–57]	0.8 ± 0.1	2.1 ± 0.3	1.9	20.4 (22.4)
Carvacrol	**CarOH**	150.2	8.32 [37]	3.3 ± 0.3 [40,48,54]	0.8 ± 0.1	2.0 ± 0.3	1.9	18.5 (20.3)
(+)-Terpinen−4-ol	**TerOH**	154.3	11.5 [38]	2.9 ± 0.4 [38,40,58]	7.4 ± 0.5	2.8 ± 0.2	1.9	17.2
Benzyl alcohol	**BOH**	108.1	323.7 [19]	1.1 ± 0.1 [47]	9.9 ± 0.7	1.5 ± 0.2	1.9	12.2 (6.3)
cyclohexanol	**CycOH**	100.2	359.4 [19]	1.2 ± 0.05 [47]	24.9 ± 0.9	1.8 ± 0.1	1.9	10.0
phenol	**PhOH**	94.1	894.7 [19]	1.5 ± 0.05 [40,47,58–61]	25.2 ± 0.9	1.5 ± 0.1	1.9	N.A.

Group 2 (intermediate water solubility) formed more complex structures like multilamellar vesicles or/and lamellar sheets, see Figure S1. The only exception is TerOH from Group 2 which has the highest solubility in 10 wt% BS from this group of 11.4 wt% and forms liquid droplets as the molecules from Group 3. Therefore, this molecule has intermediate behavior between the molecules from Group 2 and Group 3.

3.2. Effect of additive concentration on BS viscosity at fixed salt concentration of 112 mM NaCl

The rheological behavior of the BS solutions in presence of cyclic molecules at different concentrations was studied in absence of added electrolyte. Note that all systems discussed in the current section contain ≈ 112 mM NaCl coming from zwitterionic CAPB as admixture which is constant background electrolyte. The experimental data for apparent viscosity as a function of shear rate are shown in Figure S2.

The addition of Group 1 molecules (DIPB, GTPN, LMN and pCMN) results in formation of solutions with Newtonian behavior. In the whole studied concentration range of additives (between 0 and 5 wt%) the viscosity of 10 wt% BS solution decreases upon the addition of these molecules.

The addition of molecules from Group 2 (MOH, TLN, ThOH, CarOH, TerOH) to 10 wt% BS solution induces the formation of interwoven worm-like micelles (WLM) with typical non-Newtonian behavior [7]: almost constant viscosity at low shear rate, which decreases linearly with shear rate at high shear rates.

Solutions formed upon addition of non-phenolic molecules from Group 3 (BOH and CycOH) to BS have Newtonian behavior in whole concentration range and the measured viscosities passes through a maximum as a function of additive concentration. Phenol which has the highest water solubility and the highest *LogP* (1.5) from this group behaves as molecules from second group inducing the formation of interwoven micelles in a certain concentration range as can be seen from data shown in Figure S2L. Note that phenolic molecules from Group 2 (ThOH and CarOH) induces the highest increase in the apparent viscosity of BS solutions, see Figures S2G and S2H.

The experimental data shown in Figure S2 are used to construct the dependence of viscosity as a function of additive concentration, Fig. 2 and as a function of ratio between the additive and SLES molecules, Figure S3. Note that for non-Newtonian solutions the zero-shear viscosity (apparent viscosity at low shear rates) is shown in these figures.

The addition of additives from Group 1 (DIPB, GTPN, LMN, pCMN) at concentrations between 30 and 250 mM leads to decrease of BS viscosity from 10 mPa·s to 2.5 mPa·s, see Fig. 2 A. The decrease is the steepest for the most hydrophobic molecule (DIPB) and slightly weaker for GTPN and LMN, whereas the addition of 40 mM pCMN does not affect significantly the viscosity of 10 wt% BS. Further increase of pCMN concentration decrease it and the limiting viscosity of 2.5 mPa·s is reached after addition of 70 mM pCMN to 10 wt% BS. Note that water solubility of these molecules is very low, which means that the decrease of the viscosity is related to their incorporation in the BS micelles which change their properties.

The addition of molecules from Group 2 with intermediate water solubility (MOH, TLN, ThOH, CarOH and TerOH) and phenol from Group 3 (PhOH) has significant impact on the zero-shear viscosity. The maximal viscosity is reached when phenolic molecules CarOH and ThOH with relatively high *LogP* of 3.3 are used as additives. At this case the viscosity increases from 10 mPa·s to 800 Pa·s upon addition of 60 mM of these additives to 10 wt% BS. The further increase of their concentration leads to formation of non-transparent solutions as was explained in the previous section due to formation of lamellar phases, see Figure S1. The addition of alicyclic alcohol MOH with *LogP* of 3.5 at concentration of 60 mM also increases significantly the viscosity of 10 wt% BS but the maximal viscosity that is reached at this concentration is 14 Pa·s, which is 50-times lower than the viscosity of ThOH and CarOH containing BS solutions at same concentration, which means that the hydrophobic phenols are much more efficient to increase the viscosity of BS solutions compared to alicyclic alcohols. The further increase of MOH concentration does not lead to formation of turbid solutions as in the case of ThOH and CarOH, but instead the viscosity starts to decrease. The formation of turbid solution in presence of MOH is observed at concentrations above 300 mM where the long threads are well seen in the solution, see Figure S1. Other alicyclic alcohol from Group 2, TerOH with *LogP* of 2.9 also induces the growth of BS micelles but the maximal viscosity that can be reached is even lower than that reached in presence of MOH (0.5 vs 14 Pa·s). The concentration of TerOH at which this viscosity is reached is higher of ≈ 100 mM which is at least partially related to its higher solubility in water. The conclusion that the phenolic molecules are more efficient to induce the growth of BS micelles than alicyclic alcohols is supported also if one compare the effects of Phenol (*LogP*=1.5) and CycOH (*LogP* = 1.2) on BS viscosity. The addition of 160 mM PhOH increases BS viscosity up to 18 Pa·s, whereas the maximal viscosity reached in presence of CycOH is only 22 mPa·s, which is around 3-order of magnitude smaller. The replacement of OH group from phenol with methyl group in TLN also decreases the maximal viscosity that can be reached (18 vs 2.6 Pa·s).

The effect of aromatic alcohol (BOH) is also significantly smaller as compared to the effect of PhOH, but somewhat higher as compared to effect of alicyclic CycOH (40 vs 22 mPa·s) as can be seen from data shown in Fig. 2 A. Therefore, these two alcohols (BOH and CycOH) are able to induce limited growth of SLES + CAPB micelles in absence of added salt.

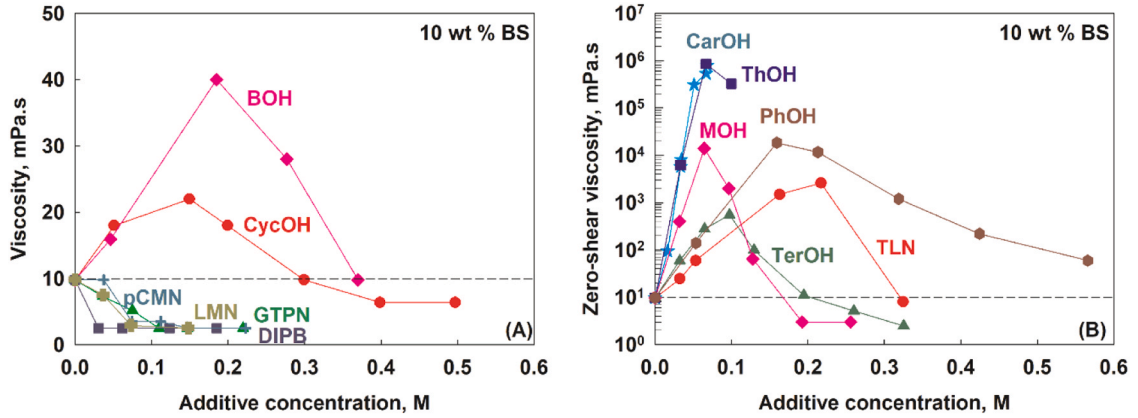

Fig. 2. (A) Viscosity for Newtonian solutions of 10 wt% BS with additives from Group 1 (DIPB, GTPN, LMN and pCMN) and non-phenolic alcohols from Group 3 (CycOH and BOH) and (B) Zero-shear viscosity for non-Newtonian solutions of 10 wt% BS with additives from Group 2 (MOH, TLN, ThOH, CarOH, TerOH) and phenol (PhOH) from Group 3 as a function of additive concentration. Note that all solutions contain 112 mM NaCl coming from CAPB.

In order to determine whether the higher required concentrations for PhOH and TLN to induce the micellar growth is related to their higher solubility in water we calculated the number of molecules incorporated in the surfactant micelles by using the partitioning coefficient between micelles and water shown in Table 1:

$$g_A^M = \frac{g_A^T}{1 + \frac{g_W}{g_S} 10^{-\text{Log}\frac{C_M}{C_W}}} \quad (1)$$

where g_A^T is the total mass of the additive added to the 10 wt% BS solution, $g_A^M$is the mass of the additive which is incorporated in surfactant micelles, g_W is the mass of water used for the preparation of a given solution. Note that the mass of water decreases with the increase of additive and salt concentrations, $g_S$is the mass of the surfactant used for preparation of the solution. The values of Log $\frac{C_M}{C_W}$ for different additives are shown in Table 1.

The experimental data from Fig. 2 are replotted as function of the ratio between the additive and SLES molecules included in micelles in Figure S3. One sees that the ratio between additive and SLES molecules in the micelles at which the molecules from Group 1 (DIPB, GTPN, LMN, pCMN) induce the significant drop in the viscosity is ≈ 0.3. At the same ratio the molecules from Group 2 and *LogP* ≈ 3.4 (MOH, ThOH and CarOH) reached the maximal viscosity, see Figure S3B, whereas the maximal viscosity is reached at ratio of 0.5 for TerOH (*LogP* = 2.9); 0.6 for PhOH (*LogP* = 1.5) and 0.75 for BOH (*LogP* = 1.1) and CycOH (*LogP* = 1.2). The ratio between TLN and SLES at which the maximal viscosity is reached for this additive is the highest ≈ 1 independently of the fact that this molecule has *LogP* = 2.6.

From this series of experiments, we can conclude that the addition of Group 1 hydrophobic molecules (DIPB, GTPN, LMN, pCMN) with *LogP* > 4.0 to 10 wt% BS solution at fixed 112 mM NaCl coming from CAPB decrease its viscosity. The molecules from Group 2 (intermediate water solubility with *LogP* between 2.6 and 3.5) induce the formation of interwoven worm-like micelles. Non-phenolic molecules from Group 3 (BOH and CycOH) increase in small extend the viscosity of BS solution, whereas PhOH which has the highest water solubility and *LogP* = 1.5 is able to induce the formation of worm-like micelles. From both Group 2 and Group 3 the most efficient for inducing growth of BS micelles are phenolic molecules: CarOH, ThOH and PhOH.

3.3. Effect of added NaCl on the rheological properties of 10 wt% BS + 0.5 wt% additive

The flow curves of 10 wt% BS and 0.5 wt% additive at varying added NaCl concentrations are presented in Figure S4. In the presence of each of the studied additives, there is a threshold NaCl concentration required for inducing worm-like micelles formation. Flow curves of solutions with worm-like micelles are characterized by two regions: an almost plateau region at low shear rates, and a viscosity decrease with a power-law index of −1 at high shear rates. As can be seen from Figure S4, for solutions containing 10 wt% BS and all studied additives, there is a concentration range of NaCl in which interwoven worm-like micelles are formed, but this concentration range differs significantly for different additives.

The zero-shear viscosity of 10 wt% BS with 0.5 wt% additive is plotted against NaCl molality in Fig. 3. At this additive concentration, all studied molecules, decrease the amount of NaCl required to reach the viscosity peak in the salt curve, as seen in Fig. 3. The maximal viscosity that is reached is higher when cyclic hydrocarbon is added to BS. Group 1 additives (DIPB, GTPN, LMN, pCMN), which were previously found to decrease the viscosity of 10 wt% BS at 112 mM NaCl, now lead to a significant increase in the maximal viscosity in a certain salt concentration range. So the effect of an additive depends not only on its concentration but also on the concentration of NaCl in BS solution.

The effect of molecules containing OH-group is mixed: they can either increase the maximal viscosity for phenolic molecules (CarOH and ThOH) with *LogP* = 3.3 or decrease it for alicyclic alcohols (MOH, TerOH, CycOH), aromatic alcohol (BOH) and simple phenol (PhOH) with *LogP* = 1.5.

The experimental data from Fig. 3 are replotted in Figure S5 as a function of total NaCl expressed in mM. These data were fitted by a Gausian equation (see Eq. (3) below) to determine three characteristics of the salt curve: the maximum viscosity, η_{max}, the total NaCl concentration required to reach the maximum viscosity, C_{MNaCl} and the width of the salt curve distribution, $C_{\sigma NaCl}$, see Table S3. As can be seen all studied additives significantly decrease both C_{MNaCl} and $C_{\sigma NaCl}$. However, the effect on maximum viscosity depends on the molecular characteristics of used additives. Hydrocarbons and hydrophobic phenols increase η_{max}, whereas alcohols and the simple phenol decrease it.

To characterize the micellar systems at salt concentrations around C_{MNaCl}, oscillatory rheological measurements were performed to determine the storage, G' and the loss, G'' moduli as a function of the frequency of oscillation, see Figure S6. The plateau modulus, G_0, and the characteristic relaxation time, τ_R, were determined from the crossover point where $G' = G''$ and are plotted in Fig. 4 as a function of scaled salt concentration, $\beta = (C_{NaCl}\text{-}C_{MNaCl})/C_{\sigma NaCl}$ [25]. Across the studied range of β (from −1.5 to +1.5), G_0 remains almost constant or increases slightly for all studied additives. The determined values of G_0 were used to calculate the micellar mesh size by using the equation [62–64]:

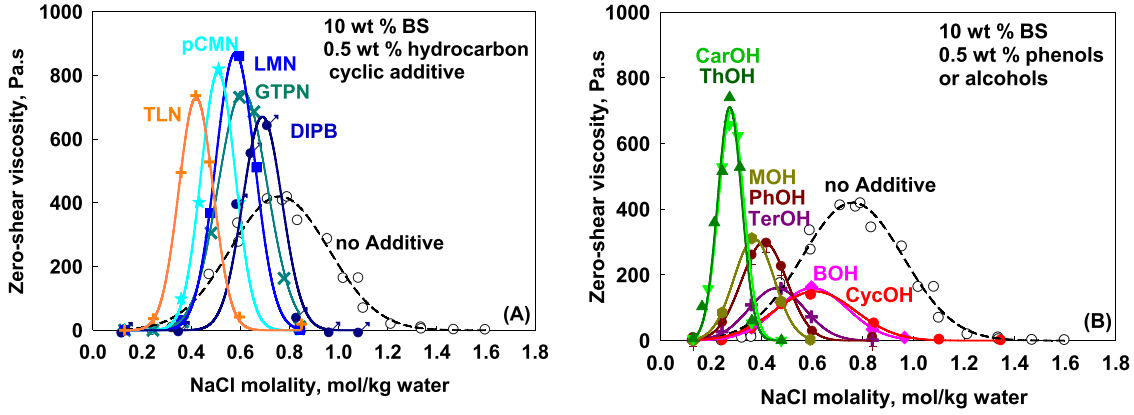

Fig. 3. Zero-shear viscosity as a function of total NaCl molality in solutions containing 10 wt% BS and 0.5 wt%: (A) Hydrocarbon cyclic additives from Group 1 (DIPB, GTPN, LMN, pCMN) and toluene (TLN) from Group 2; (B) Additives possessing hydroxyl group from Group 2 (MOH, ThOH, CarOH, and TerOH) and Group 3 (BOH, CycOH and PhOH). The points are experimental data, whereas the curves are best fit of data with Gaussian distribution, which describes well the data around the maximum.

$$\xi = \left(\frac{k_B T}{G_0}\right)^{1/3}$$

where k_B is the Boltzmann constant and T is the temperature. The calculated mesh size is $\xi = 31 \pm 2$ nm for all studied systems within the studied range of β. This constant mesh size confirms that the viscosity decrease observed beyond the salt curve maximum is not driven by a significant shortening of the micelles, but is instead governed by micellar branching.

The relaxation time obtained from the crossover frequencies are presented in Fig. 4B. The relaxation time is substantially shorter for systems containing alcohols than for those with hydrophobic phenols and cyclic hydrocarbons, while the simple phenol exhibits intermediate behavior. This accelerated relaxation behavior for alcohols and simple phenols is in excellent agreement with the lower maximum bulk viscosities determined from their respective salt curves.

The experimental data from Figure S6 are reploted in Figure S7 as Cole-Cole plot (G''/G_0 vs G'/G_0). The experimental data closely follow the ideal Maxwellian behavior represented by the continuous semi-circularcurve in Figure S7. This means that the studied systems are within fast-breakaing regime, where the reptation time, τ_{REP}, associated with the curvilinear movement of the wormlike micelles through the entangled network is significantly longer than the breakage time, τ_{BR}, which is due to the breakage and recombination of micellar segments [65,66]. This behavior is characteristic of interwoven wormlike micellar networks and further confirms that the primary mechanism driving the viscosity decrease beyond the salt curve maximum is micellar branching rather than shortening.

In conclusion, a reduction in the required NaCl concentration to reach peak viscosity is a common effect for twelve tested cyclic additives. However, their specific impact on the magnitude of the maximum viscosity of BS solution depends on their chemical structure. The peak viscosity is enhanced by the addition of cyclic hydrocarbons (DIPB, GTPN, LMN, pCMN and TLN) and by hydrophobic phenolic molecules with a relatively high hydrophobicity of *LogP* = 3.3 (CarOH and ThOH), while the maximum viscosity is reduced by the incorporation of alicyclic alcohols (MOH, TerOH, CycOH), an aromatic alcohol (BOH) and simple phenol (PhOH).

3.4. Effect of additive concentration on the salt curves

The performed experiments at fixed additive weight concentration show that the additives have different impact on the salt curves, as seen form Fig. 3. However, the number of additive molecules incorporated in the surfactant micelles varies due to their molecular masses and partitioning coefficients between the aqueous phase and the micelles. To determine the effect of the additive concentration on the salt curves, we performed experiments with four additives (TLN, PhOH, CycOH and BOH) at 0.3 wt% concentration in 10 wt% BS solution. The experimental results from these experiments are shown in Figure S8.

The obtained salt curves are shown in Fig. 5, along with the experimental data for the respective additive at 0.5 wt%. The results at 0.3 wt % concentration consistently lie between the data obtained without additive and the data obtained in the presence of 0.5 wt% additive. For examples, the addition of TLN at 0.5 wt% increases the maximal viscosity of the 10 wt% BS solution. Consequently, the maximal viscosity determined in the presence of 0.3 wt% TLN is lower than that measured at 0.5 wt% toluene (560 vs 730 Pa·s), but higher than the viscosity measured for 10 wt% BS solution (420 Pa·s). An opposite behavior is observed for the other three tested additives, which upon their addition at 0.5 wt% to 10 wt% BS, decrease the maximal viscosity.

All different additives decrease the required salt concentration needed to reach the maximal viscosity, as shown in Table 5 and as a consequence, for all of them, a higher concentration of NaCl is required to reach the maximal viscosity when 0.3 wt% additive is used instead of 0.5 wt%.

3.5. NMR

In order to gain more detailed information about the position of studied molecules in the BS micelles we performed NMR experiments (^{1}H NMR and ^{13}C NMR).

3.5.1. BS micelles (no additives)

The comparative ^{1}H NMR analysis of the individual surfactants, CAPB and SLES, and their mixture shows the formation of mixed micelles by examining the behavior of both the hydrophobic tails and the polar head groups, see Figure S9.

The NMR signals from the hydrophobic alkyl tails of both surfactants show clear mixing. There are several peaks for the methyl protons of SLES appearing between 0.78 ppm and 0.86 ppm with the highest peak being at 0.84 ppm. In ^{1}H NMR spectra of CAPB the presence of several peaks is also seen with the highest appearing at 0.84 ppm. In BS micelles all these peaks appear as one broader peak instead of individual ones, see Figure S9D. This indicates effective mixing of the non-polar tails. Similarly, the methylene protons in the hydrophobic tail of SLES and CAPB are well mixed and one merged peak is detected for the hydrophobic tail methylene protons of the mixture, unambiguously confirming the formation of mixed micelles.

Analysis of the polar head group regions demonstrates specific intermolecular interactions. The NH proton signal of CAPB is significantly affected, it shifts from 8.14 ppm (CAPB alone) to 7.80 ppm (BS), which is related to NH protons surrounded by the CH2 groups of the SLES ethoxy chain, placing them in a relatively more hydrophobic

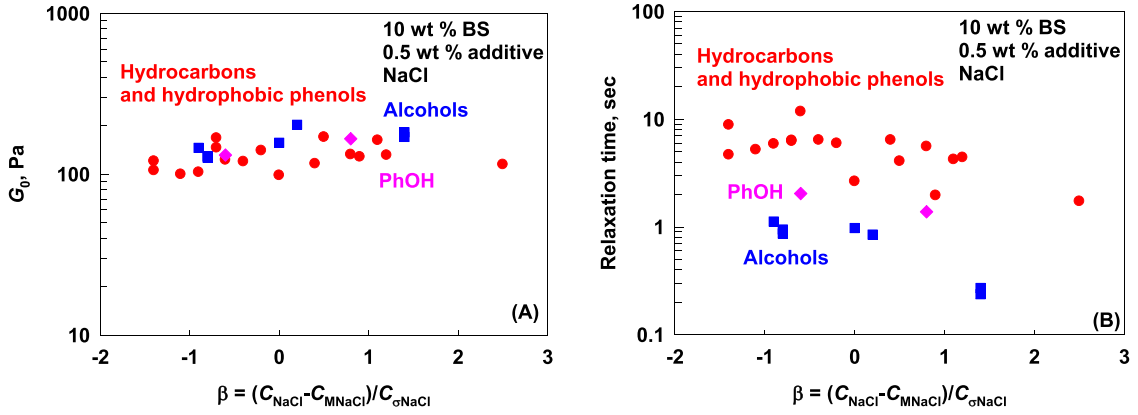

Fig. 4. (A) Elasticity, G_0, as determined from oscillatory experiments and (B) relaxation time, τ_R as a function of scaled salt concentration, β= (C_{NaCl}-C_{MNaCl})/$C_{σNaCl}$ for solutions containing 10 wt% BS + 0.5 wt% additive at different salt concentrations.

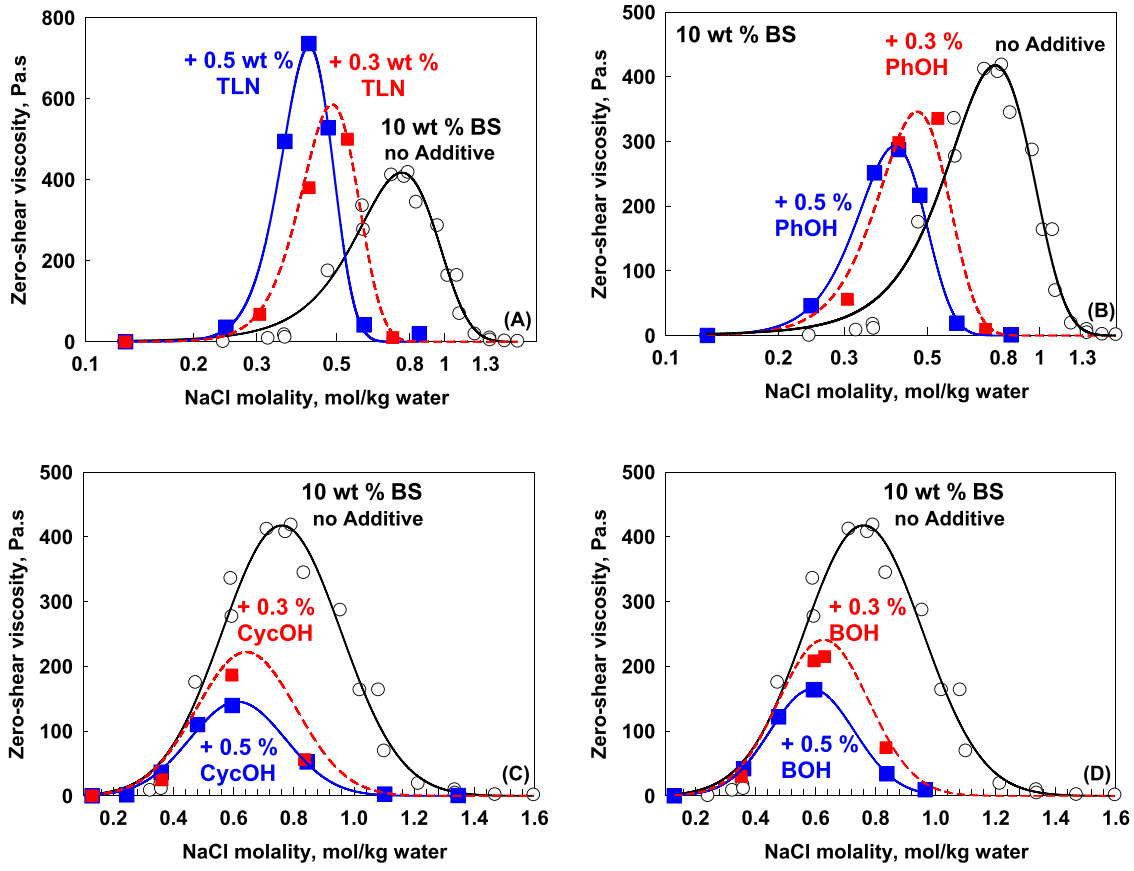

Fig. 5. Zero-shear viscosity as a function of total NaCl molality in solutions containing 10 wt% BS and 0.5 wt% (blue symbols) and 0.3 wt% (red symbols): (A) Toluene; (B) Phenol; (C) Cyclohexanol; (D) Benzyl alcohol. The points are experimental data, whereas the continuous curves are best fit of data with Gaussian distribution, which describes well the data around the maximum. The dashed red curves are predicted dependences based on Gaussian distribution with values of η_{max}, m_{max}, m_σ determined from Eqs. (4)-(6) below.

environment. This finding is supported by the behavior of the SLES ethoxy protons, which appear as multiple peaks in SLES and merge in two broad peaks in BS.

The ^{13}C NMR data confirms significant structural reorganization within the mixed micelles, see Table 2 below and Figure S10. The carbon atoms from the methyl groups of SLES are upfield shifted by 2.6 Hz. This indicates that these hydrophobic termini are now in a more shielded, non-polar environment due to effective mixing with the hydrophobic tails of CAPB. A similar upfield shifting is determined for the carbon atom in the amide group of CAPB, suggesting that this part of the CAPB molecule is surrounded by the hydrophobic part of the SLES molecule, pulling this region into a more shielded environment. In contrast, the carbon atom from the CH2 group attached to NH in the propyl part of CAPB is significantly downfield shifted by 127 Hz. This deshielding indicates that this part of the CAPB molecule is surrounded by the hydrophilic part of SLES, specifically the ethoxy groups. Supporting this interaction, the carbon atoms from the ethoxy groups of SLES are upfield shifted after mixing with CAPB, showing they are in close proximity to the less polar propyl chain of the CAPB molecule. Finally, the signal for the carbon from the COO− group in CAPB is also significantly downfield shifted by 66 Hz. The upfield shifting of C-atoms from CH3 groups attached to positively charged N-atom in CAPB with 65 Hz show that these atoms are in less polar environment because positively charged N-atom is partially neutralized by negatively charged sulfate group of SLES which decreases the polar environment around CH3 groups attached to positively charged N-atom in CAPB, see Fig. 6.

3.5.2. BS micelles with 1 wt% additives (at 112 NaCl)

In an attempt to identify the localization of the studied molecules in the surfactant micelles, we performed NMR analysis of BS and mixtures of BS with additives at higher additive concentration of 1 wt% for three of the molecules from Group 1 (GTPN, LMN, pCMN) and two of the molecules from Group 2 (ThOH and TerOH) without added electrolyte.

Proton NMR spectroscopy was used to evaluate the impact of the additive on the chemical environment of the surfactants. Although we can detect a change in the chemical shift of the additive signals before and after their incorporation into the micelles, due to the very low concentration of the additive relative to the surfactant molecules, no significant chemical shift is observed in most of the main BS signals (see Fig. 7 and Figure S11). Only in the presence of 1 wt% pCMN we detect

Table 2
Chemical shift of particular carbon signals in ^{13}C NMR spectra of the BS system, compared to the individual SLES and CAPB.

Additive	CH3 (1) from SLES	CH3 (2) from CAPB	$(CH3)_2N$ (3) from CAPB	CH_2-NH (4) from CAPB	CH2-O (5) from SLES	CH2-O (6) from SLES	COO^- (7) from CAPB	CON (8) from CAPB
SLES	13.92				67.47	68.71		
CAPB		13.99	51.36	62.16			168.70	178.80
BS, Δ, Hz	−2.6	−1.4	−65.0	+ 127.0	−18.3	−4.4	+ 66.0	−6.5

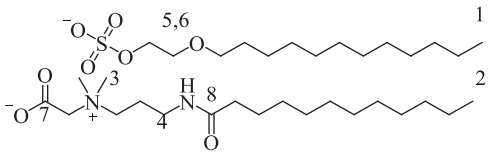

Fig. 6. Spatial distribution of SLES and CAPB in BS micelles (no NaCl).

some shift in the spectra for the H-atoms in CH_3 groups attached to the quaternary N with 6 Hz. Also, the signal from H-atoms in CH_2 close to COO^- is shifted in the presence of pCMN by 8 Hz, while in the presence of ThOH, this signal is shifted by 12 Hz. The N-H signal of CAPB is shifted in the presence of TerOH by 12 Hz, and in the presence of ThOH by −42 Hz. This indicates the special proximity of the additive to the NH, possibly due to hydrogen bonding, since those are the only additives bearing hydroxyl group. Note that hydroxylic group in ThOH is much more acidic as compared to TerOH which can explain the chemical shift towards lower frequencies.

To further understand the molecular mechanisms underlying the rheological behavior and salt curve modulation observed in BS systems containing various cyclic additives, we applied ^{13}C NMR spectroscopy to selected samples. These measurements allowed us to probe the local microenvironment around the carbon atoms of the surfactant system in the presence of different additives and to indicate the most probable localization of the additives within the micellar structure.

The comparison between the ^{13}C NMR spectra of additive-containing BS systems and the reference BS solution (without additive) revealed specific chemical shift changes (Δ) that can be interpreted as indicators of additive–surfactant interactions, see Tables 3, 4 and S4 and Fig. 8.

In the presence of GTPN, a notable shift of approximately 4 Hz was observed in the aliphatic region of the spectrum, particularly for carbon atoms corresponding to –CH_3 groups in the surfactant tails. No significant change was observed in the headgroup region of CAPB, except for the signal of CON group, which is shifted by 7.5 Hz. Most of the signals in the head region of SLES are not shifted with more than 1 Hz, except for the signal at 68.67 ppm which is shifted by 5.4 Hz. This indicates that GTPN interacts preferentially with the hydrophobic core of the micelles. This is consistent with its high hydrophobicity, low polarity, and absence of polar functional groups, which together favor its incorporation into micellar core.

Similarly, LMN caused slight shift in the signals for CH_2 of the tail regions and terminal methyl group (~4 Hz), implying a position within the core of the micelle. The signal at 63.17 coming from CAPB head group (CH_2NH) is slightly shifted by 3 Hz towards lower frequencies, whereas the C-atom from carboxylic groups and C-atom attached to quaterny N-atom in CAPB are almost not affected. Therefore, LMN is also preferentially situated in the core of the micelles.

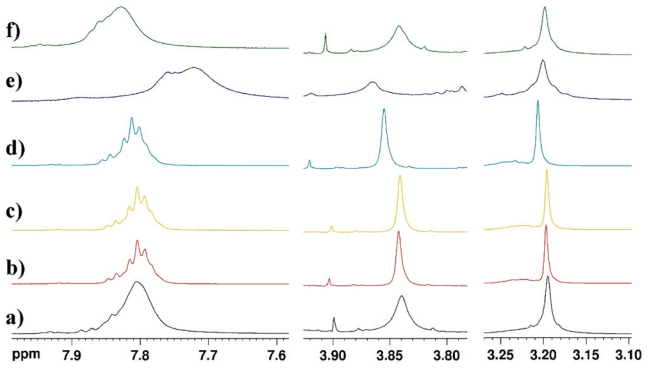

Fig. 7. Representative regions of ^1H NMR spectra of the BS system with and without additives: (A) BS (black); (B) BS + 1 wt% GTPN (red); (C) BS + 1 wt% LMN (yellow); (D) BS + 1 wt% pCMN (cyan); (E) BS + 1 wt% ThOH (dark blue); (F) BS + 1 wt% TerOH (dark green).

pCMN induced chemical shift changes in the CH_3 groups region (shifts of ~5.2 Hz) but not in the CH_2 signals. The signal of CON group is shifted by 11 Hz, and the signal at 68.67 ppm by 8.0 Hz. The difference between pCMN and the two aforementioned additives is observed in the change of the headgroup region of CAPB for the signal of the two methyl groups attached to the quaternary N, for which pCMN induces a shift by 4.4 Hz, which means that this molecule is positioned between the core of the palisade layer of the micelles.

The ^1H NMR spectrum provides additional evidence that pCMN is solubilized between the core and palisade layer of the BS micelles. When pCMN is incorporated into the BS system, all its characteristic proton peaks undergo a significant upfield shift. This shift means the pCMN protons are experiencing increased electron shielding when solubilized inside the micelles compared to their environment in a typical organic solvent. For instance, the isopropyl methyl protons, which normally appear as a doublet near 1.2 ppm, are strongly shifted upfield to 0.99 ppm. Similarly, the aromatic methyl singlet, typically found at 2.5 ppm, is significantly affected by the presence of the BS micelles, shifting upfield to 2.02 ppm, again showing that these protons are much better shielded inside the micelle core. Further confirmation comes from the aromatic protons (two doublets) which shift from the expected 7.0 −7.2 ppm range to approximately 6.8 ppm (Table 4.).

The ^{13}C NMR spectrum of BS in presence of TerOH show that the most affected are the signals of the C-atoms in the heads of CAPB – $(CH_3)_2N$ by 4.9 Hz and CH_2NH by −8 Hz. The methyl groups are more shielded and are shifted with −3.2 Hz. There are some changes in the C-atoms of the tails and of the C-atoms of SLES-heads both by 3 Hz. After this analysis we can conclude that TerOH is located in the palisade layer and affect the core of the micelles by changing the packing parameter. The characteristics peaks for protons from TerOH that appear at 0.92 ppm are not significantly shifted when TerOH is incorporated in BS micelles which also supports the conclusion that TerOH is situated in the palisade layer of the micelles. However, the peak from vinylic proton (H−C═C), next to the methyl group on the ring which appears at 5.37 ppm is shifted to 5.26 ppm which means that this part of the molecule is close to the core of the micelles.

The most pronounced NMR effects were observed for ThOH. It produced notable shifts in the headgroup region, particularly within the ethoxylated chains of SLES (10–11 Hz) and the CAPB headgroup (~10/−10 Hz). These shifts indicate strong interactions with the micellar shell, most likely via hydrogen bonding involving phenolic group. ThOH, in particular, caused extensive perturbation of headgroup carbons without significantly altering tail signals, suggesting exclusive localization within the palisade layer of the micelles. This behavior aligns with its planar aromatic structure, which enhance headgroup packing and promote the formation of highly viscous wormlike micelles (WLMs).

Table S5 summarizes the chemical shifts of selected carbon atoms in the BS system upon addition of ThOH at two different concentrations (0.3 wt% and 1 wt%). The data reveal a clear trend of increasing chemical shift perturbation with increasing ThOH concentration, particularly in the headgroup regions. At 0.3 wt% ThOH, only minor changes are observed, with shifts of less than 4 Hz in most regions. However, when the concentration is increased to 1 wt%, significant shifts occur—most notably in the ethoxylated CH_2O groups of SLES (~12 Hz) and in the carbonyl (CON) region of CAPB (~20.5 Hz). These shifts suggest stronger interactions between ThOH and the polar headgroups of both surfactants at higher additive levels.

Despite the increased magnitude of chemical shift changes, it is important to note that signal quality worsens with higher ThOH content, as indicated by broader peaks in the 1 wt% spectrum. This is due to poor magnetic field homogeneity (shimming issues), compounded by increased solution viscosity and possible microheterogeneity introduced by the additive. As a result, some carbon signals become less well-resolved at higher additive concentrations.

Taken together, these results confirm that ThOH primarily interacts

Table 3
Chemical shift of particular carbon signals in ^{13}C NMR spectra of the BS system with and without 1 wt% additives, compared to BS. The number in the parenthesis indicates the specific carbon atom as shown in Fig. 8.

Additive	CH3 (1) from SLES	CH3 (2) from CAPB	$(CH3)_2N$ (3) from CAPB	CH_2-NH (4) from CAPB	CH2-O (5) from SLES	CH2-O (6) from SLES	COO (7) from CAPB	CON (8) from CAPB
BS, ppm	13.90	13.95	50.84	63.17	67.32	68.67	169.20	175.75
BS + GTPN, Δ, Hz	4.2	3.9	1.3	−1.3	3.0	5.4	1.2	7.5
BS + LMN, Δ, Hz	3.9	3.4	0	−3.2	1.1	3.7	−0.9	6.2
BS + pCMN,Δ, Hz	5.2	5.8	4.4	0.9	3.9	8.0	1.9	11.0
BS + ThOH*,Δ, Hz	3.9	1.8	10.8	−11.5	12.0	11.0	0	20.5
BS + TerOH,Δ, Hz	−3.2	−3.6	4.9	−7.9	3.0	0.3	−1.6	0

* Broad signals due to bad shimming

Table 4
Suggested position of the additives in the BS-micelles and respective the most important shifts.

BS System + 1% additive:	Chemical shifts induced by the presence of additive (^1H NMR)	Chemical shifts induced by the presence of additive (^{13}C NMR)	Chemical shifts in the ^1H NMR for protons from the additive	Suggested position of the additive in the micelles
GTPN	No Changes in the chemical shift	CH_3 – 4 Hz, SLES heads – 3/5 Hz.	$(CH_3)_2$ – −26 Hz CH_2 – −26 Hz CH= – −27 Hz	Core of the micelles
LMN	No Changes in the chemical shift	CH_3 – 3–4 Hz, Heads of SLES 1–4 Hz	CH_3 – −32 Hz CH_2= – −35 Hz CH= – −35 Hz	Core of the micelles
pCMN	CH_3 – - 10 Hz $N(CH_3)_2$ – 6 Hz CH_2COO – 8 Hz NH – no change CH_2(head) – 5 Hz	Shift in the tails CH_3 - 5 Hz, Heads of SLES 4–8 Hz, CAPB CON – 11 Hz.	$(CH_3)_2$ – 102 Hz CH_3 – 123 Hz PhH – 104 Hz	Between core and palisade layer
ThOH	CH_3 – 26 Hz $N(CH_3)_2$ – 3 Hz CH_2COO – 13 Hz NH – - 41 Hz CH_2O – changes	Shift in the heads of SLES −11–12 Hz CAPB – 11/ −11.5 Hz, CAPB CON−11Hz.	$(CH_3)_2$ – −6 Hz CH_3 – −23 Hz PhH(s) – 29 Hz PhH(d) – 143 Hz	Palisade layer
TerOH	CH_3 – - 4 Hz $N(CH_3)_2$ – 2 Hz CH_2COO – 1 Hz NH – 12 Hz CH_2(tail) – - 5 Hz	Shift in the heads of CAPB 5/−8Hz, SLES 1–3 Hz.	$(CH_3)_2$ – −7 Hz CH_3 – −16 Hz CH= – −57 Hz	Palisade layer

with the headgroup regions of the micelles and that its effect is concentration-dependent. The observed chemical shift changes at higher loading correlate with the previously discussed rheological behavior—namely, a substantial increase in viscosity due to tighter packing of the surfactant headgroups and enhanced micellar structure.

3.6. SAXS measurements

To evaluate structural changes in the micellar cross-section, the experimental SAXS scattering curves, shown in Figure S12, were analyzed using a model-independent approach. The data were converted from reciprocal space to real space via Inverse Fourier transform implemented in the SasView software package. The normalized pair distance distribution functions (PDDF) are shown in Fig. 9. For the wormlike micellar structures investigated here, the cross-section of PDDF profile provides a direct measure of the local radial dimensions. The micellar core radius R_c was determined unambiguously from the real-space position where the primary electronic density correlation crosses the abscissa. This zero-crossing point is governed intrinsically by the contrast step between the scattering length densities (SLD) of the hydrophobic core and the hydrophilic shell, eliminating the requirement to know SLD values of core and shell. The determined core radii (R_c) are summarized in Table 1. The results indicate that molecules from Group 1 (DIPB, GTPN, LMN, and pCMN) significantly increase the core radius of BS micelles from 1.9 nm to 2.2 nm. Hydrocarbon (TLN) from Group 2 induces only a small increase to 2.0 nm, while all other molecules from Groups 2 and 3 have no detectable effect on the core radius. These results show that hydrocarbon molecules are primarily solubilized within the micellar core. On the hand, all phenols and alcohols reside within the palisade layer or at the micelle surface and core radius is unchanged.

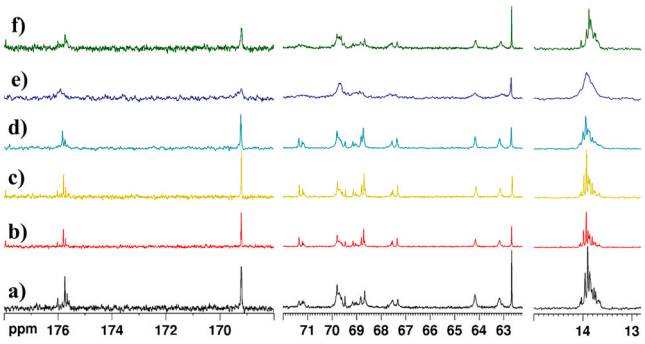

Fig. 8. ^{13}C NMR spectra of the BS system with and without additives for signals associated with methyl groups of the surfactant tails−12–15 ppm; EO- groups of the SLES−62–72 ppm; head groups from CAPB – 169–172 ppm for: (A) BS (black); (B) BS + 1 wt% GTPN (red); (C) BS + 1 wt% LMN (yellow); (D) BS + 1 wt% pCMN (cyan); (E) BS + 1 wt% ThOH (dark blue); (F) BS + 1 wt% TerOH (dark green).

3.7. Effect of studied additives on interfacial properties of dodecane-water

The packing of the molecules within the micelles strongly depends on the hydrophobic attraction between the hydrophobic tails and repulsions between the hydrophilic groups. It was shown in the previous sections that hydrocarbon molecules from Group 1 and Toluene from Group 2 are incorporated in the core of the micelles, whereas the hydrophobic phenols and alcohols from Group 2 are situated in the palisade layer of the micelles. To test how the studied additives, affect the interfacial tension of dodecane-water interface we measured the interfacial tension in presence of 10 mol% of studied additives in the dodecane. All prepared oily solutions are transparent and stable over

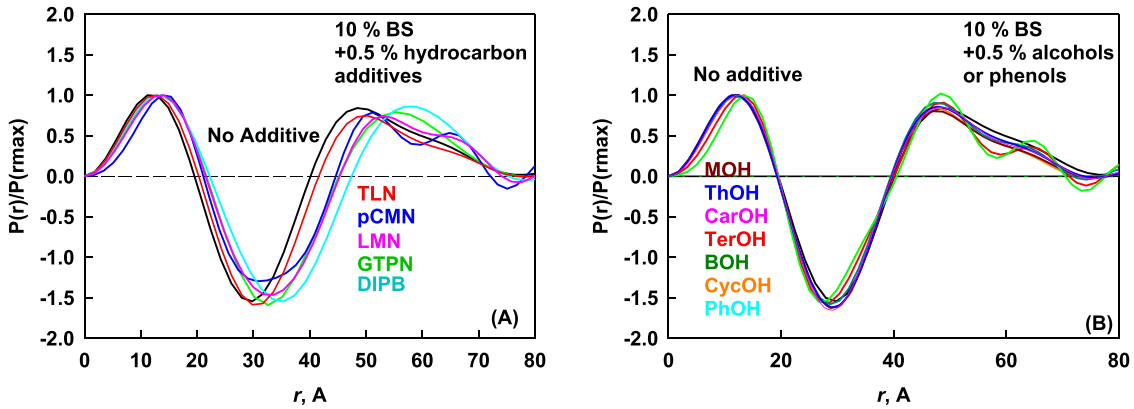

Fig. 9. Pair-distance distribution functions derived via Inverse Fourier transform with SasView software for 10 wt% BS in presence of 0.5 wt% additives of: (A) Hydrocarbons and (B) Alcohols and phenols.

time with the exception of those prepared with the molecules from Group 3 (high water solubility) – BOH and PhOH. The benzyl alcohol phase separated from dodecane as oily drops, whereas phenol phase separates as crystals. The decrease of the concentration of studied additives to 5 mol% does not change the phase behavior of dodecane solutions of additives from Group 3. Therefore, the additives from Group 3 are incorporated in the palisade layer and around the surface of the micelles because they do not mix with dodecane at the concentrations at which they are incorporated in the BS micelles. Molecules from Group 1 and Group 2 are well soluble in dodecane and can be incorporated in the micelles. As shown from NMR and SAXS analysis the molecules from Group 1 are incorporated in the core of the micelles, whereas the molecules from Group 2 are in palisade layer (the exception is TLN).

The measured interfacial tensions are shown in Fig. 10 and interfacial tensions determined after 900 s are summarized in Table 1 above. All studied additives decrease the interfacial tension of dodecane-water interface which is measured to be 52.0 mN/m in good agreement with literature data [67]. The decrease is the largest for additives from Group 3 which are able to decrease the interfacial tension of dodecane-water interface from 52 mN/m down to 12 mN/m. Hydrophobic phenols from Group 2 decrease the interfacial tension from 52 mN/m down to 17 mN/m (TerOH) and 18.5 mN/m (CarOH), whereas alcohols from the same group decrease it to 20.4 mN/m (ThOH) and 23 mN/m (MOH). Interestingly the similar significant decrease in IFT is measured also for LMN, which does not possess OH-group and belongs to Group 1. This molecule decreases the interfacial tension down to 15.4 mN/m. On the other hand, GTPN is not able to decrease so efficiently the interfacial tension and the measured value is 30.8 mN/m. The main difference between LMN and GTPN is related to the fact that two double bonds in GTPN are located in the ring and the molecule cannot adsorb efficiently on dodecane-water interface, whereas one of the two double bonds in LMN is located outside the ring and it can rearrange on the dodecane-water interface by decreasing significantly unfavorable contacts between water and dodecane. Other molecules from Group 1 decrease the interfacial tension from 52 mN/m down to 39.4 mN/m (p-CMN) and to 33.4 mN/m (DIPB). The smallest decrease is determined for TLN, for which the measured interfacial tension is 47.4 mN/m showing that this molecule prefers to stay inside the dodecane and not adsorbing on the water-dodecane surface.

4. Data interpretation and discussion

4.1. *Effect of additives on main characteristics of salt curve*

Based on the experimental results presented in Figs. 2–5, it is seen that the effect of additives on BS micelles depends on the concentrations of both the additive and the added salt. To quantitatively determine how the molecular properties of the studied additives affect the BS micelles, the following approach was used: (1) The molar fraction of the additive incorporated into the BS micelles, x_A^M was determined by Eq. (2); (2) Three main characteristics of the salt curves: the maximal viscosity, η_{max}, the molality of NaCl required to reach the maximal viscosity, m_{max} and the width of salt curve, m_σ were determined from the best fit of experimental data with Gaussian distribution, Eq. (3); (3) The dimensionless parameters (s_A – characterizing the ability of molecules to decrease the molality of NaCl required to induce WLM formation in BS+additive solutions, p_A - accounting for change in the width of salt curve upon additive addition and k_A -accounting for the change in the maximal viscosity that can be reached upon additive addition) characterizing the ability of a given additive to affect the main characteristics of the salt curve (m_{max}, η_{max}, m_σ) were determined from dependences of m_{max}, η_{max} and m_σ on x_A^M; (4) The dependences of the dimensionless parameters (s_A, p_A, k_A) on the molecular properties (molecular volume of

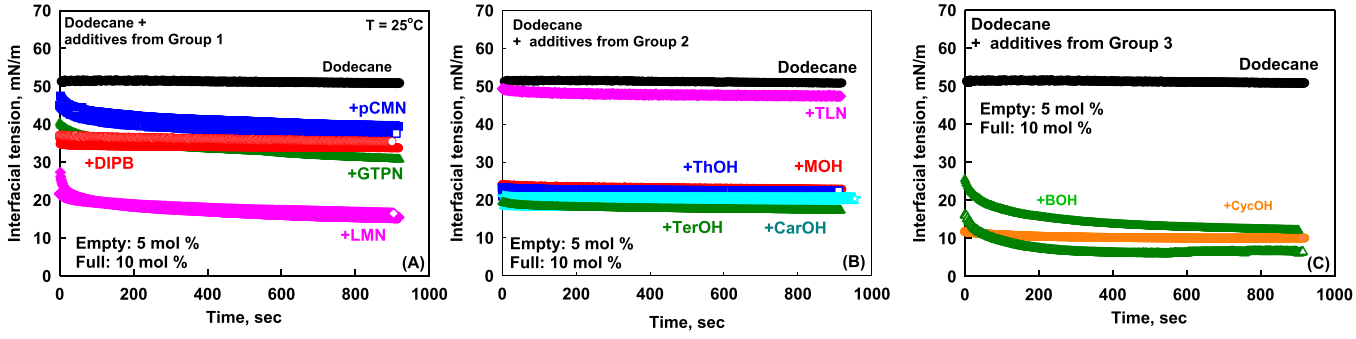

Fig. 10. The interfacial tension of dodecane-water as a function of time for dodecane containing 5 mol% (empty symbols) or 10 mol% full symbols of studied additives from (A) Group 1 (low water solubility); (B) Group 2 (intermediate water solubility) and (C) Group 3 (high water solubility).

additive and its *LogP*) are established and discussed. All the determined parameters are summarized in Table 5.

4.1.1. Molar fraction of the additive incorporated into the BS micelles

The molar fraction of the additives in BS micelles is calculated by using the following expression:

$$x_A^M = \frac{g_A^M / M_A}{g_A^M / M_A + g_{SLES} / M_{SLES} + g_{CAPB} / M_{CAPB}} \quad (2)$$

Where g_A^M is determined from Eq. (1), M_A is the molar mass of different additives, which are given in Table 5, g_{SLES} is the mass of SLES used for solution preparation, M_{SLES} is its molecular mass which is 332.4 g/mol and g_{CAPB} is the mass of CAPB used for solution preparation and M_{CAPB} is its molecular mass, which is 342.52 g/mol. The calculated molar fraction of added additives in the surfactant micelles varies between 0.092 for CarOH to 0.153 for TLN for 10 wt% BS solutions prepared with 0.5 wt% additive concentration.

4.1.2. Main characteristics of salt curves

The maximal viscosity, η_{max}, the molality of NaCl required to reach the maximal viscosity, m_{max} and the width of salt curve, m_σ were determined by empirical fitting of the experimental data shown in Fig. 3 and 5 by Gaussian equation [68,69]:

$$\eta = \eta_{max} \exp\left(-\frac{(m_{NaCl} - m_{max})^2}{2m_\sigma^2} \right) \quad (3)$$

Where m_{NaCl} is the molality of NaCl in the mixture (it accounts for the added NaCl as background electrolyte and the presence of NaCl in CAPB solution). The similar approach is used to fit the experimental data as a function of electrolyte concentration instead of molarity and the respective values from the best fit are shown in Table S3. The determined values of η_{max}, m_{max} and m_σ are shown in Table 5. It is seen that all additives decrease m_{max} and m_σ as compared to values determined for 10 wt% BS without additives, whereas the value of η_{max} in presence of additive could be higher or lower as compared to value determined for 10 wt% BS (no additive). It is seen also that the determined characteristics for a given additive depend on their molar fraction in the micelles – see data in Table 5 in parentheses for four additives for each we performed the experiments at two concentrations.

4.1.3. Dependences of main characteristics of salt curves on molar fraction of the additive incorporated into the BS micelles

The values of m_{max} (the molality of NaCl required to reach the maximal viscosity) decrease as a function of the molar fraction of the additive incorporated in the micelles, x_A^M, for all studied additives, see Table 5. The results revealed a linear dependence between m_{max} and $\sqrt{x_A^M}$, as shown in Fig. 11. This relationship can be expressed as:

$$\frac{m_{max\ ,BS+A}}{m_{max\ ,BS}} = 1 - s_A \sqrt{x_A^M} \quad (4)$$

Here $m_{max,BS+A}$ is the molality of NaCl required to reach the maximal viscosity in BS + Additive solution at x_A^M, $m_{max,BS}$ is the molality of NaCl required to reach maximal viscosity for BS solution without additive, which is 0.76 and s_A is the slope of linear dependence of $\frac{m_{max\ ,BS+A}}{m_{max\ ,BS}}$ vs $\sqrt{x_A^M}$. The dimensionless parameter s_A characterizes the ability of additive molecules to decrease the molality of NaCl needed to induce the formation of interwoven worm-like micelles in BS + additive solutions.

The determined values of s_A are given in Table 5. It is seen that s_A varies between 0.30 (DIPB) and 1.0 (p-CMN) for additives in Group 1. The values of s_A are higher for all molecules in Group 2 varying between 1.1 (TLN) and 2.1 (ThOH and CarOH). The determined values of s_A for molecules from Group 3 range between 0.6 (CycOH) and 1.3 (PhOH).

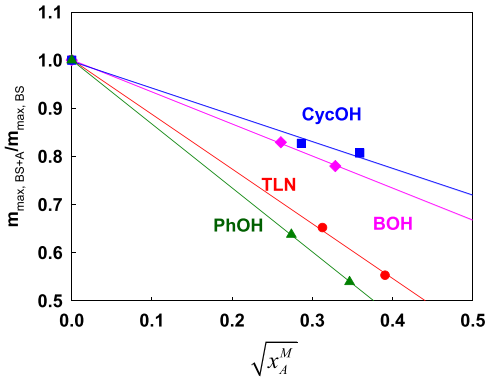

Fig. 11. Scaled molality of NaCl required to reach the maximum viscosity for BS solutions with additive, $m_{max,BS+A}$ and without additive, $m_{max,BS}$ as a function of square root of molar fraction, of additive in BS micelles for PhOH (green triangles); TLN (red circles); BOH (pink diamonds) and CycOH (blue squares).

Table 5

Partitioning coefficient octanol-water, *LogP*, molecular volume, v_A, fraction of a given additive in the BS micelles, x_A^M, maximal viscosity in salt curve, η_{max}, molality of NaCl required to reach maximal viscosity, m_{max}, the width of salt curve distribution, m_σ. The values for x_A^M, η_{max}, m_{max} and m_σ are determined from salt curves of 10 wt % BS + 0.5 wt% additive, whereas the data in parentheses are determined from salt curves of 10 wt% BS + 0.3 wt%. The dimensionless parameters: s_A accounting for decrease of salt concentration to reach the maximal viscosity, k_A accounting for the change in the maximal viscosity that can be reached upon additive addition and p_A which accounts for change in the width of salt curve upon additive addition.

Additive	*Log P*	v_A, mL/mol	x_A^M	η_{max}, Pa·s	m_{max}, mol/kg	m_σ, mol/kg	s_A	k_A	p_A
-	-	-	0	420 ± 15	0.76 ± 0.01	0.20 ± 0.008	-	-	-
DIPB	5.3 ± 0.1	189.3	0.094	670 ± 40	0.69 ± 0.01	0.08 ± 0.008	0.3 ± 0.05	2.8 ± 0.5	1.8 ± 0.3
GTPN	4.5 ± 0.2	160.5	0.110	750 ± 15	0.61 ± 0.01	0.10 ± 0.002	0.6 ± 0.05	2.8 ± 0.5	1.2 ± 0.3
LMN	4.6 ± 0.2	162.0	0.110	870 ± 15	0.58 ± 0.01	0.08 ± 0.001	0.7 ± 0.05	3.6 ± 0.5	1.4 ± 0.3
pCMN	4.1 ± 0.1	156.6	0.111	810 ± 15	0.51 ± 0.01	0.07 ± 0.001	1.0 ± 0.1	2.8 ± 0.5	1.5 ± 0.3
MOH	3.5 ± 0.3	171.2	0.096	310 ± 25	0.37 ± 0.01	0.08 ± 0.001	1.7 ± 0.1	−2.4 ± 0.5	0.5 ± 0.5
TLN	2.6 ± 0.2	106.8	0.153	730 ± 15	0.42 ± 0.01	0.07 ± 0.002	1.1 ± 0.1	1.0 ± 0.2	1.0 ± 0.5
			(0.098)	(560 ± 20)	(0.50 ± 0.01)	(0.09 ± 0.005)			
ThOH	3.3 ± 0.2	154.9	0.094	710 ± 45	0.28 ± 0.01	0.05 ± 0.004	2.1 ± 0.1	1.3 ± 0.2	1.0 ± 0.4
CarOH	3.3 ± 0.3	153.8	0.092	700 ± 45	0.28 ± 0.01	0.05 ± 0.004	2.1 ± 0.1	1.3 ± 0.2	1.0 ± 0.4
TerOH	2.9 ± 0.4	166.6	0.097	160 ± 15	0.46 ± 0.01	0.11 ± 0.004	1.3 ± 0.1	−7.0 ± 0.5	0.2 ± 0.2
BOH	1.1 ± 0.1	103.8	0.108	160 ± 15	0.60 ± 0.01	0.14 ± 0.003	0.7 ± 0.05	−8.5 ± 1.5	0.3 ± 0.3
			(0.068)	(210 ± 15)	(0.63 ± 0.01)	(0.14 ± 0.001)			
CycOH	1.2 ± 0.05	104.2	0.129	150 ± 15	0.61 ± 0.01	0.16 ± 0.006	0.6 ± 0.05	−8.0 ± 1.5	0.1 ± 0.1
			(0.082)	(190 ± 15)	(0.63 ± 0.01)	(0.13 ± 0.001)			
PhOH	1.5 ± 0.05	89.2	0.120	300 ± 15	0.41 ± 0.01	0.09 ± 0.002	1.4 ± 0.05	−2.3 ± 0.3	0.6 ± 0.3
			(0.075)	(390 ± 15)	(0.48 ± 0.01)	(0.09 ± 0.002)			

The maximal viscosity, η_{max}, reached in the presence of additives depends on the type of molecule, which controls whether the viscosity will be higher or lower than that of the BS solution (420 Pa·s). The molar fraction of the additive incorporated in the BS micelles is also important. To determine the dimensionless parameter, k_A, which accounts for the effect of additive on the maximal viscosity in the salt curve we used the following approach: (1) Determine the maximal relative viscosity, which is a ratio between the maximal viscosity obtained in the presence of additive at the molar fraction of x_A^M in the micelles, η_{max}^{BS+AD} and maximal viscosity for 10 wt% BS solution without additive, η_{max}^{BS} which is 420 Pa·s. (2) Account for the higher total surfactant concentration included in the surfactant micelles in presence of additive by dividing the relative maximal viscosity on $(1+x_A^M)^2$. The value of power law index of 2 is used because in our previous study we showed [25] that for worm-like micelles, the maximal viscosity in salt curve increases with the increase of the surfactant concentration to the power of 2.0 in the presence of monovalent ions [25]; (3) Account for different molality of NaCl that is required to reach maximal viscosity in presence of studied additives. Note that the different NaCl molality at the salt curve maximum means that the fraction of neutralized SLES molecules in the micelles is different which affects the bending ability of the micellar fragments and might change the branching ability of micelles. The following expression is used to determine the dimensionless parameter k_A which characterize the ability of additives to change the maximal viscosity in salt curve:

$$\frac{\eta_{max}^{BS+A}}{\eta_{max}^{BS}} = (1+x_A^M)^2 \exp\left(k_A \frac{x_A^M}{1-s_A\sqrt{x_A^M}}\right) \quad (5)$$

Where η_{max}^{BS+AD} is the maximal viscosity obtained in the presence of additive at the molar fraction of x_A^M in the micelles, η_{max}^{BS} is the maximal viscosity for 10 wt% BS solution without additive, which is 420 Pa·s. The parameter k_A accounts for the effect of different additives on the maximal viscosity that can be reached. Note that the parameter k_A is positive for additives that increase the maximal viscosity and negative for those that decrease it. The predicted maximal viscosities for solutions with 0.3 wt% additive, are compared with the experimentally measured values in Figure S13. A good agreement is established, which confirms that Eq. (5) can correctly predict the maximal viscosities for BS solutions formed in the presence of an additive molar fraction in the micelles up to 0.15 at least for four studied additives for which the salt curve are measured at two different additive concentrations.

The determined values of k_A are shown in Table 5. The values of $k_A \approx 2.8 \pm 0.5$ for Group 1 (DIPB, GTPN and pCMN) and only for LMN which shows stronger ability to decrease the interfacial tension, the value of $k_A \approx 3.6 \pm 0.5$ is slightly higher. The values of k_A for Group 3 are negative and vary between −2.3 (PhOH) and −8.5 (BOH). Hydrophobic phenols (ThOH and CarOH) and toluene (TLN) from Group 2 have positive values of $k_A \approx 1.2$, whereas alcohols (MOH and TerOH) have negative values of −2.4 and −7.0 showing that alcohols decrease the maximal viscosity, whereas hydrophobic phenols increase it.

To determine the dimensionless parameter, p_A, that accounts for effect of additive on the width of salt curve we determined the dimensionless width distribution by calculating the ratio between width of salt curve BS + additive, $m_{\sigma,BS+A}$, and width for salt curve of BS $m_{\sigma,BS} = 0.20$. Then we account for the fact that the higher value of m_{max} usually leads to higher value of m_σ, see Figure S14 and that is why we divide the normalized width distribution to normalized maximal molality expressed by Eq. (4). The following equation was used to determine the dimensionless parameter, p_A, which accounts for contribution of additives to the width of the salt distribution:

$$\frac{m_{\sigma,BS+A}}{m_{\sigma,BS}} = \left(1-s_A\sqrt{x_A^M}\right)\left(1-p_A\sqrt{x_A^M}\right) \quad (6)$$

where $m_{\sigma,BS+A}$ is the width of the salt curve for BS + additive at the molar fraction of additive in the micelles of x_A^M, $m_{\sigma,BS}$ is the width of salt curve for BS solution without additives, which is set at 0.20. The first term in the right-hand side of the equation accounts for the effect of additive on the molality of NaCl required to reach the maximal viscosity, whereas the second term accounts for additional contribution of the additive on the width of salt curve. The parameter p_A characterizes the ability of additive molecules to decrease further the width of salt curve except of their effect to decrease the value of m_{max}, which in its own turn decreases significantly m_σ. The determined values of p_A are shown in Table 5.

The values of parameter $p_A \approx 1.5 \pm 0.3$ for Group 1 showing that these molecules further decrease the width of salt curve distribution beyond their effect on the m_{max}. The values of $p_A \approx 1.0 \pm 0.3$ for TLN, CarOH and ThOH are determined for Group 2, which increase the maximal viscosity, whereas all alcohols from Group 2 and Group 3 have value of p_A which is very close to 0 showing the decreased value of $m_{\sigma,BS+A}$ for these additives is mainly related to their effect on m_{max}.

To test the validity of the determined values of s_A, k_A and p_A we calculate the dependences for salt curve in presence of 0.3 wt% for four additives for which we measured these dependences. The predicted dependencies are shown in Fig. 5 as dashed lines. It is seen that they agree well with experimental data showing that this approach can be used for additive molar fractions in the range between 0 and 0.15. The proposed approach described adequately the viscosities around the maximum in the salt curve.

It should be mentioned that the low viscosities at low NaCl concentrations are not well described by Gaussian distribution as was shown in our previous studies [7,25] and in that case four characteristic parameters should be used for proper description of the whole salt curve. However, for most of studied additives we do not have enough data at low salt concentrations and that is why we cannot determine the effect of studied additives on the salt curve shape at low salt concentrations.

4.2. Relation between dimensionless parameters and molecular properties of studied additives

As can be seen from data presented in Table 5, the values of the dimensionless parameters exhibit a clear dependence on *LogP*. However, when these parameters are plotted directly as a function of *LogP*, the results for molecules with smaller molecular volume such as TLN, PhOH, BOH, and CycOH noticeably deviate from the general trend, see Figure S15. Using micelle-water partition coefficient, $\mathrm{Log}(C_M/C_W)$ instead of *LogP*, does not improve the correlation and lower regression coefficients are determined, as shown in Figure S15. To accurately account for the varying molecular sizes of the additives, in Fig. 12 we plotted the dimensionless parameters as a function of $v_{BS}/v_A LogP$. The volume of SLES + CAPB surfactant molecules is set at $v_{BS} = 0.577$ nm^3 [25] and v_A is the molar volume of the additives listed in Table 5.

It is seen that s_A increases with $v_{BS}/v_A LogP$ for phenols and alcohols, whereas it decreases for hydrocarbon additives. This different behavior arises from the different positioning of these molecules within the surfactant micelles. Hydrocarbons incorporate into the micellar core, increasing the core radius as shown in Fig. 9. Because they are positioned close to the core of the micelles, they cannot sufficiently reduce the electrostatic repulsion between the charged SLES headgroups.

In contrast, molecules containing hydroxyl groups, such as alcohols and phenols, do not change the micellar core radius. Instead, they are incorporated in the palisade layer or stay on the micellar surface. This positioning allows them to significantly modulate the repulsion between charged headgroups. An increase in *LogP* for these additives enhances their efficiency in screening SLES repulsions, because more hydrophobic molecules exhibit lower water solubility and prefer to remain at the micellar interface between the charged SLES molecules. Furthermore, a decrease in the molecular volume of the additives increases their screening efficiency. This effect is observed because smaller molecules

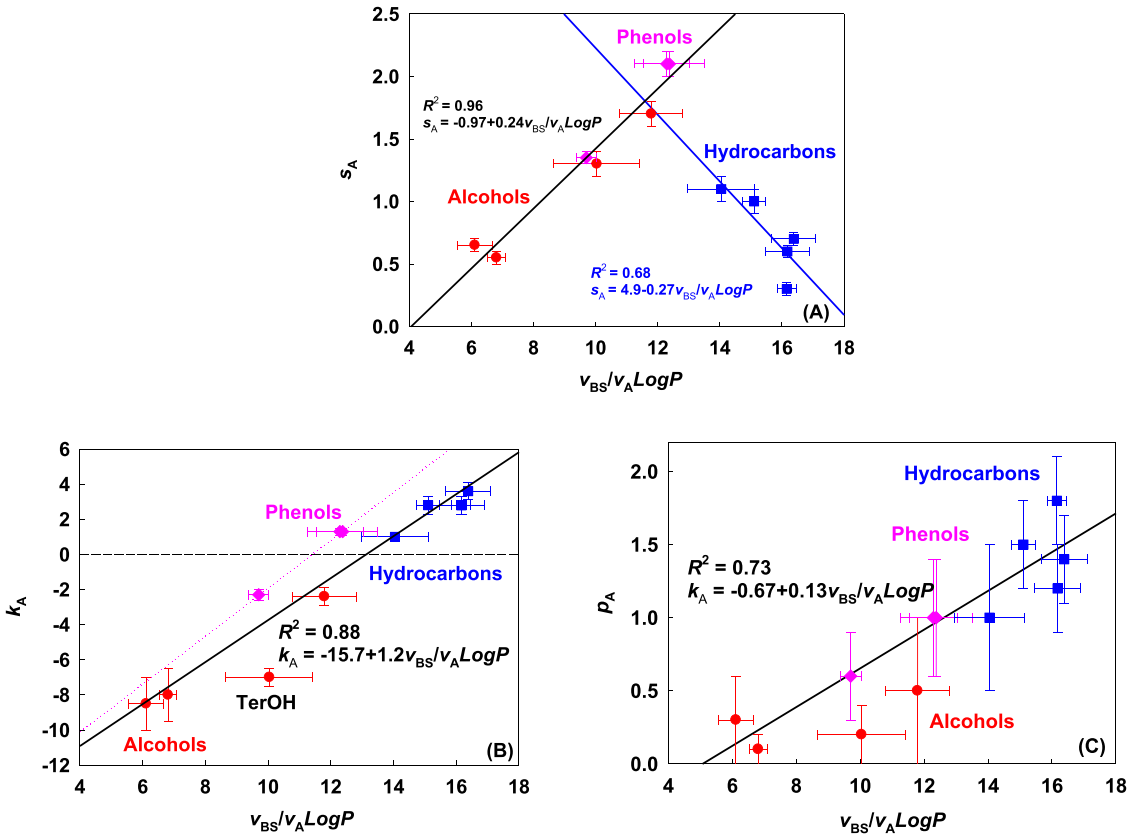

Fig. 12. Dimensionless parameters as a function of the ratio between the volume of SLES and volume of additive multiply by *LogP* value: $v_{SLES}/v_A LogP$ for: (A) The dimensionless parameter s_A accounting for the decrease of molality of NaCl required to reach the maximal viscosity in the salt curve of 10 wt% BS upon addition of different additives; (B) The dimensionless parameter k_A accounting for the effect of additive on the maximal viscosity that can be reached in the salt curve of 10 wt% BS as a function multiply by s_A and (C) The dimensionless parameter p_A accounting for the change in the width of the salt curve upon additive addition in 10 wt% BS solutions.

occupy less average surface area at the micellar interface, leading to more effective charge mitigation.

The dependence of k_A, which accounts for the effect of additives on peak viscosity, on $v_{BS}/v_A LogP$ is presented in Fig. 12B. It is seen that k_A is a linear function of $v_{BS}/v_A LogP$ for both hydrocarbons and alcohols. The only significant deviation from this linear trend is observed for TerOH, which reduces the maximum reachable viscosity to a greater extent than predicted by its molecular characteristics. This behavior is attributed to its inability to form strong hydrogen bonds with surfactant molecules. Note that TerOH has the lowest melting point (–63°C) among all studied hydroxyl-containing additives, further indicating its weak hydrogen-bonding capacity. Phenols also deviate from the linear dependence, but they lie above the curve. Such molecules form stronger hydrogen bonds than alcohols and might decrease the branching ability of the BS micelles. The data show that hydrocarbon and alcohol additives with $v_{BS}/v_A LogP < 13$ decrease the maximum viscosity of 10 wt% BS, whereas the threshold value for phenols is lower, at approximately 11.5. The general increase of k_A with $v_{BS}/v_A LogP$ can be explained by the facilitated branching of micelles when using additives with low *LogP*. Such molecules redistribute more easily into the high-curvature regions of branched micelles, thereby decreasing the free energy penalty associated with branching. In contrast, the stronger hydrogen bonds formed by phenols hinder their redistribution into these curved regions and branching becomes more difficult, resulting in higher observed viscosities in the presence of these additives.

The linear dependence between p_A, which accounts for effect of additives on the width of salt curve, and $v_{BS}/v_A LogP$ is obtained for all studied additives, showing that the width of distribution decreases significantly with the increase of additives hydrophobicity, which means that thermolecules that are incorporated inside the micellar core can form the worm like micelles only on very narrow concentration of NaCl in the solution.

4.3. *Effect of additives on BS micelles at 112 mM NaCl*

Group 1 (DIPB, GTPN, LMN, and pCMN) do not increase the viscosity of a 10 wt% BS solution at 112 mM NaCl coming from CAPB. This behavior is attributed to their high lipophilicity as seen by their high *LogP* > 4.0. These molecules exhibit very low water solubility but are highly soluble in dodecane. As confirmed by NMR and SAXS analysis, these molecules are positioned within the hydrophobic core of the micelles. Consequently, they are unable to screen the electrostatic repulsions between the charged SLES molecules at the micellar surface at 112 mM NaCl. Without this charge screening, micellar growth is inhibited, and the solution maintains a low viscosity.

The addition of molecules from Group 2 (MOH, TLN, ThOH, CarOH, and TerOH), to a 10 wt% BS solution results in a significant viscosity increase within a certain concentration range, followed by viscosity decrease at higher concentrations at 112 mM NaCl. The peak viscosity is reached at specific additive/SLES molar ratios that correlate directly to the *LogP* value of the used molecules. For molecules MOH, ThOH, and CarOH, with a *LogP* between 3.3 and 3.5, the maximal viscosity occurs at a ratio of approximately 0.33. This requirement increases to 0.44 for TerOH, (*LogP* = 2.9), and reaches 1.00 for TEN, (*LogP* = 2.6). This trend shows that as *LogP* decreases, a higher additive-to-surfactant ratio is necessary to reach peak in the viscosity. This can be explained with specific position of these molecules within the palisade layer. NMR data further clarifies this behavior by showing that while both ThOH and

TerOH are incorporated in the palisade layer, their effect on the relative positioning of SLES and CAPB molecules differs significantly. Thymol induces a more pronounced effect on the packing of the hydrophobic tails, indicating that it is firmly anchored within the micelle. In contrast, TerOH is more water-soluble and resides closer to the micellar surface, making it more prone to detachment. Similarly, MOH remains firmly attached due to its high *LogP* and low water solubility. The variation in peak viscosity between the alcohols (MOH and TerOH) and hydrophobic phenols (ThOH and CarOH) is primarily driven by the strength of hydrogen bonding. The stronger H-bonds formed by hydrophobic phenols stabilize the micellar assembly and this might prevent their branching, whereas the weaker H-bonds formed by alcohols lead to a much lower viscosity. Toluene, which lacks a hydroxyl group, shows low affinity for the interface of the micelles and it stays in the core of the micelles as shown from SAXS data and that is why it affects only slightly viscosity at low concentrations. The effect becomes significant when its molar fraction increases and it positions between the head groups of the surfactants.

Group 3 (BOH, CycOH, and PhOH) are distinguished by their ability to induce structural changes in the micelles. Phenol is capable of inducing the formation of worm-like micelles, whereas benzyl alcohol and cyclohexanol are not. The latter two additives significantly reduce the dodecane-water interfacial tension, confirming their position at the interface between the aqueous phase and the micellar surface. Despite their impact on headgroup interactions, their high-water solubility causes them to desorb easily from the micelles, which explains why their effect on viscosity is less pronounced than that of Group 2 molecules. The better performance of phenol compared to CycOH and BOH is fundamentally related to the stronger hydrogen bonds it forms with the surfactant headgroups. This enhanced bonding decreases the probability for phenol detaching from the micellar surface. Consequently, phenol promotes micellar growth and increases solution viscosity to a much greater extent than the alcohols in this group in absence of background electrolyte.

The schematic representation of proposed mechanisms for three groups of studied cyclic molecules in presence and absence of salt is shown in Fig. 13.

4.4. Comparison of our experimental data with data from the literature

The work of Tang et al. [18] describes the effect of 15 perfume molecules on the zero-shear viscosity of a body wash (BW−1) formulation, which contains 8.85 wt% SLES1EO, 1.15 wt% CAPB, 0.7 wt% NaCl, and a 1 wt% perfume mixture. The effect of additional 15 mM of specific perfume molecules along with of the existing mixture was studied and the results were explained by using *LogP* of the additives [18]. Molecules with an intermediate *LogP* of approximately 3.3, such as benzyl benzoate and cumene, were found to increase the BW−1 viscosity by 40%, increasing it it from 11 Pa·s to 15 Pa·s. Molecules with *LogP* of 2.4 (linalool) or those ranging between 3.59 and 4.71, including florhydral, beta-ionone, D-Limonene, and terpinolene, did not significantly affect the viscosity. For molecules with lower *LogP* values between −0.61 (dipropylene glycol) and 1.73 (triethyl citrate), a decrease in viscosity was observed. This reduction was attributed to the molecules partitioning at the micellar surface, which increases the area per molecule and disrupts the packing. Molecules with a high *LogP* above

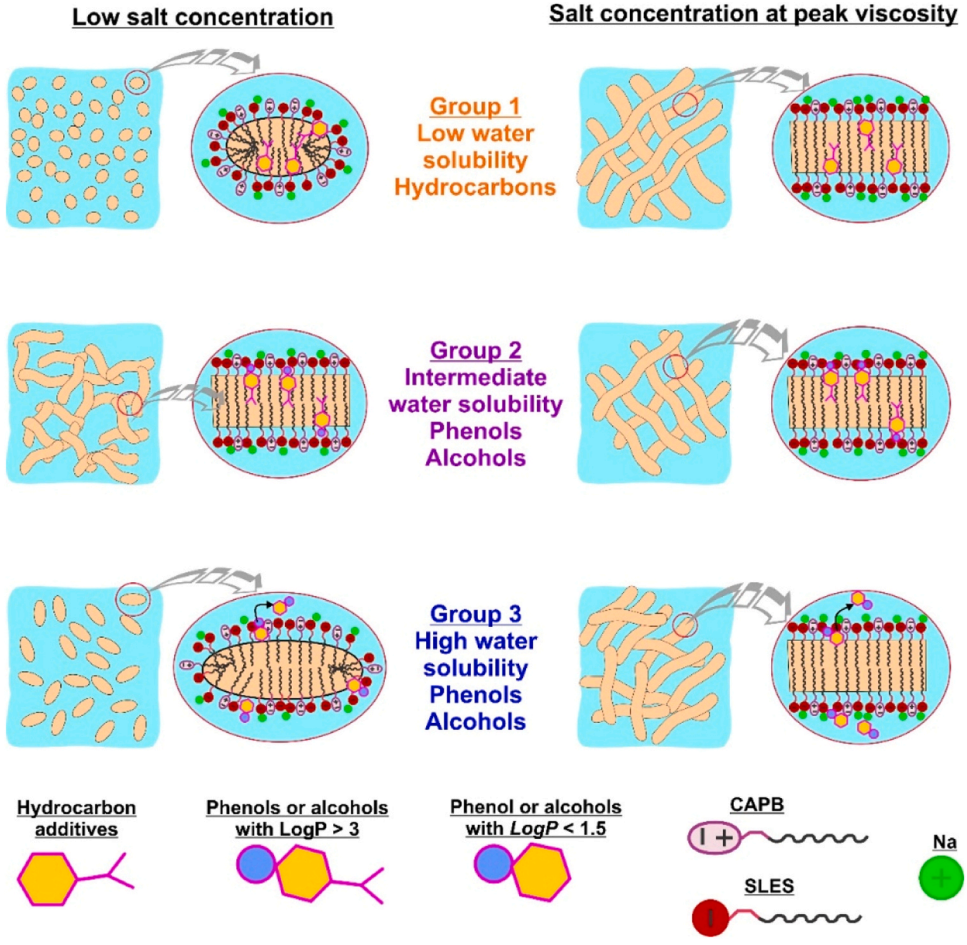

Fig. 13. Type of aggregates formed in 10 wt% BS solutions at low salt concentrations (left column) and at salt concentration inducing peak viscosity in the salt curve (right column) upon addition of additives from Group 1 (first row), Group 2 (second row) and Group 3 (third row).

4.7, such as linalyl isobutyrate, muscone, helvetolide, and isopropyl myristate, also decreased the viscosity. However, this effect was explained by their partitioning into the micelle core, which increases the effective tail length and favors the formation of smaller spherical micelles over elongated ones.

Direct comparison of results reported by Tang et al. [18] with the present study will be difficult because their base formulation contained an initial 1 wt% perfume mix, which fundamentally changes the baseline viscosity of the surfactant system. Nevertheless, the results are qualitatively consistent with our results. Both studies indicate that molecules with intermediate *LogP* values have the most significant impact on viscosity at low salt levels. Our research further extends these findings by demonstrating that high *LogP* molecules can significantly increase the viscosity of SLES1EO + CAPB formulations within specific salt concentration ranges. This behavior was not observed in the Tang et al. [18] study because their experiments were conducted at a fixed salt concentration located before the viscosity maximum.

Parker and Fieber [5] studied the effect of 0.5 wt% vanillin, linalool, citronellol, and limonene on rheological properties of 10 wt% SLES system. Their study demonstrated that linalool and citronellol significantly reduce the salt concentration required to reach maximum viscosity compared to vanillin and limonene. These findings align with our observations, where alcohols and hydrophobic phenols possessing intermediate *LogP* values exhibit the most pronounced effect on reducing the salt concentration needed for peak viscosity, as illustrated in Fig. 12. The calculated $v_{SLES}/v_a LogP$ values for the additives studied by Parker and Fieber [5] are 5.65 for vanillin, 9.55 for linalool, 12.4 for citronellol, and 16.38 for limonene. According to our model, the greatest reduction in the salt concentration required for maximum viscosity should be observed for citronellol, followed by linalool and limonene, with vanillin having the smallest effect, see Fig. 12A above. This theoretical ranking is in very good agreement with the experimental data presented in Ref. [5]. The observed impact of these molecules on the magnitude of the maximum viscosity in Ref. [5] again agrees well with our results. The largest decrease in peak viscosity was measured for vanillin, followed by linalool and citronellol [5]. These three molecules possess values below the threshold of 13.0, which we have identified as the minimum value required to induce a viscosity increase, as shown in Fig. 12B. In contrast, the addition of limonene was shown to increase the maximum viscosity of the 10 wt% SLES system [5]. This is consistent with our findings, as limonene has a $v_{SLES}/v_a LogP$ greater than 13, leading to a viscosity increase in the 10 wt% BS system as well. Consequently, the approach proposed in the current study proves to be a robust tool for assessing the effects of various additives not only for 10 wt% SLES + CAPB system, but also for 10 wt% SLES solutions.

Kamada et al. [15] investigated the effect of 0.5 wt% additives on the rheological behavior of 10 wt% SDS + C12EO3 mixtures. Their experimental results demonstrated that the maximum achievable viscosity decreases upon the addition of L-menthol, α-terpineol, geraniol, 1-decanol, and 9-decen−1-ol. Furthermore, these specific additives reduce the molar fraction of C12EO3 at which this maximum viscosity occurs. This behavior aligns with our results, where L-menthol was shown to decrease both the salt concentration required to reach peak viscosity and the magnitude of the peak viscosity itself. In contrast, the addition of D-limonene presents a different rheological profile: while it also decreases the molar fraction of C12EO3 required to reach peak viscosity, it simultaneously increases the value of the peak viscosity [15]. The similar behavior decreasing the salt concentration while increasing the peak viscosity, is also consistent with the results observed in current study, see Fig. 3A above.

McCoy et al. [19] studied the impact of various additives, including toluene, cyclohexanol, phenol, and benzyl alcohol, on the properties of 10 mM oleyl amidopropyl betaine (OAPB). Their results showed that toluene exhibits significantly higher solubility in OAPB micelles compared to other hydrocarbons like heptane and methylcyclohexane, a phenomenon they attributed to π-π interactions between the double bond in the surfactant tail and the benzene ring of the toluene. Our study also reveals that the maximum viscosity for BS system in precence of toluene occurs at a much higher surfactant-to-additive ratio than other studied hydrocarbons, see Figure S3. However, since our surfactants are saturated, the explanation provided by McCoy et al. [19] regarding tail-ring interactions is inapplicable. Instead, our results suggest that the low interfacial activity of toluene drives the molecule to reside primarily within the micellar core. McCoy et al. [19] found that cyclohexanol and benzyl alcohol had a negligible effect on the rheological response of 10 mM OAPB, whereas phenol exerted a significant impact. These observations align with our results, where phenol successfully induced the formation of wormlike micelles in 10 wt% BS without added salt, while cyclohexanol and benzyl alcohol prompted only limited micellar growth. The lack of a measurable effect from the latter two additives in the work of McCoy et al. [19] is likely due to their surfactant concentration being 20 times lower than that used in our current study. The substantial viscosity increase triggered by phenol is attributed by McCoy et al. [19] to its high proton-donating propensity, which screens the charge of the OAPB carboxylic group. We have demonstrated that this mechanism remains valid for SLES + CAPB mixtures and is even more pronounced with more hydrophobic phenols such as ThOH and CarOH. These compounds are capable of forming complex response structures similar to those previously shown by McCoy et al. [19].

The effect of 20 different additives on the phase inversion temperature (PIT) of Brij30/octane/water system was studied by Ontiverosa et al. [70]. It was shown that the most efficient molecules to decrease the PIT are phenol and thymol, whereas menthol and benzyl alcohol are much less efficient, which is explained with the different ability of hydrogen donor/acceptor capability of the therminal group. This affects the interactions between surfactant molecules on the oil-water interface, which agrees well with our explainations about the ability of phenols to form stronger H-bonds as compared to alcohols. Kanei et al., showed that linear molecules (Linalool, Geraniol and Eugeniol) with terminal hydroxyl group penetrate in the palisade layer and act as cosurfactant in nonionic surfactant system [71], whereas limonene is incorporated within the core of the micelles which agrees with our explanations.

Therefore, the obtained experimental results agree well with results from the literature and provide the theoretical framework under which these findings can be interpreted by accounting not only for their partitioning coefficient but also for the ratio between the surfactant molecular volume and molecular volume of studied additives.

5. Conclusions

The impact of twelve cyclic molecules on the micellar properties of a mixed sodium dodecyl ether sulfate and cocoamidopropyl betaine surfactant system (BS) was investigated. The studied additives are categorized into three groups. Group 1 consists of aromatic (Diisopropyl benzene and p-cymene) and alicyclic hydrocarbons (γ-Terpinene and Limonene) all of which exhibit low aqueous solubility. As demonstrated by NMR and SAXS measurements, these molecules are incorporated within the hydrophobic core of the micelles. They do not increase the viscosity of BS solution at 112 mM NaCl, but they affect the salt curve by increasing the peak viscosity, reducing the salt concentration required to achieve that peak, and narrowing the width of the salt curve. Group 2 includes Toluene, two alcohols (Menthol and Terpinenol) and two hydrophobic phenols (Thymol and Carvacrol) which have intermediate water solubility. All molecules in this group increase the viscosity of BS solutions within a specific concentration range even at 112 mM NaCl. However, their effects on the salt curve depend on their chemical structure. Hydrophobic phenols along with Toluene, increase the maximal viscosity, whereas alcohols decrease it. The higher viscosity of phenols-containing systems compared to alcohols is attributed to the formation of stronger hydrogen bonds which significantly lower the salt required to reach the peak viscosity which in its own turn increases the micellar charge density and inhibit the branching of worm-like micelles.

Group 3 includes molecules with high-water solubility: Benzyl alcohol, Cyclohexanol, and Phenol. These additives reduce the salt content required to reach peak viscosity, but they all lead to a decrease in the maximal viscosity itself. This reduction is explained by their positioning at the micellar surface and their relatively high mobility, which allows for easier redistribution and reduces the energetic penalty for micellar branching.

To quantify these effects, the experimental results were fitted to determine three dimensionless parameters: k_A which accounts for changes in maximal viscosity, s_A which represents the reduction in salt content required to reach that peak and p_A which describes the effect of additive on the width of the salt curve distribution. All these parameters were found to depend on octanol/water partitioning coefficient, *LogP* and the ratio between volumes of surfactants and the additive, v_{BS}/v_A. The parameter s_A decreases as $v_{BS}/v_A LogP$ increases for hydrocarbon additives, whereas it increases with $v_{BS}/v_A LogP$ for alcohols and phenols. A linear dependence was established between k_A and $v_{BS}/v_A LogP$. This dependence passes through zero when $v_{BS}/v_A LogP \approx 13$ for alcohols and hydrocarbons and ≈ 11.5 for phenols indicating that alcohols and hydrocarbons with $v_{BS}/v_A LogP < 13$ will decrease the maximal viscosity of BS system, whereas those with $v_{BS}/v_A LogP > 13$ will increase it. Finally, the salt width parameter, p_A also showed a dependence on $v_{BS}/v_A LogP$, demonstrating that an increase of $v_{BS}/v_A LogP$ leads to significant narrowing of the salt curve.

Future research will extend the developed approach from individual cyclic molecules to complex mixtures. Additionally, the methodology will be tested on aliphatic molecules, which represent another major fraction of essential oils, thereby broadening the scope and applicability of the current model. Complementary molecular dynamics simulations are currently underway to determine the precise orientation and partitioning behavior of the additive molecules within the surfactant aggregates. These simulations will reveal how their incorporation modulates the micellar surface charge and packing density, providing a deeper mechanistic explanation of their impact.

CRediT authorship contribution statement

Zlatina Mitrinova: Methodology, Investigation, Validation, Formal analysis, Visualization, Writing – original draft. **Nevena Pagureva:** Investigation, Formal analysis. **Nikola Burdzhiev:** Investigation, Formal analysis, Writing – review & editing. **Slavka Tcholakova:** Supervision, Methodology, Formal analysis, Conceptualization, Project administration, Funding acquisition, Writing – review & editing.

Funding

This study is financed by the European Union-Next Generation EU, through the National Recovery and Resilience Plan of the Republic of Bulgaria, project N№ BG-RRP−2.004–0008-C01.

Declaration of Competing Interest

The authors declare that they have no known competing financial interests or personal relationships that could have appeared to influence the work reported in this paper.

Acknowledgments

The support of the Centre of Competence “Sustainable Utilization of Bio-resources and Waste of Medicinal and Aromatic Plants for Innovative Bioactive Products” (BIORESOURCES BG), project BG16RFPR002–1.014–0001, funded by the Program “Research, Innovation and Digitization for Smart Transformation” 2021–2027, co-funded by the EU, is greatly acknowledged. Authors are grateful of Mrs. Stefani Paskova for performing some of the microscope observations and rheological measurements and Mrs Dora Dimitrova and Elena Kostova for performing interfacial tension measurements.

Appendix A. Supporting information

Supplementary data associated with this article can be found in the online version at doi:10.1016/j.colsurfa.2026.141166.

Data Availability

Data will be made available on request.

References

[1] L. Abezgauz, K. Kuperkar, P.A. Hassan, O. Ramon, P. Bahadur, D. Danino, Effect of Hofmeister anions on micellization and micellar growth of the surfactant cetylpyridinium chloride, J. Colloid Interface Sci. 342 (2010) 83–92.
[2] C. Oelschlaeger, P. Suwita, N. Willenbacher, Effect of Counterion Binding Efficiency on Structure and Dynamics of Wormlike Micelles, Langmuir 26 (10) (2010) 7045–7053.
[3] M.I. Alkschbirsa, A.M. Perceboma, W. Loha, H. Westfahl Jr, M.B. Cardosob, E. Sabadinia, Effects of some anions of the Hofmeister series on the rheology of cetyltrimethylammonium-salicylate wormlike micelles, Colloids Surf. A Physicochem. Eng. Asp. 470 (2015) 1–7.
[4] Z. Wang, P. Li, K. Ma, Y. Chen, J. Penfold, R.K. Thomas, D.W. Roberts, H. Xu, J. T. Petkov, Z. Yan, D.A. Venero, The structure of alkyl ester sulfonate surfactant micelles: The impact of different valence electrolytes and surfactant structure on micelle growth, J. Colloid Interface Sci. 557 (2019) 124–134.
[5] A. Parker, W. Fieber, Viscoelasticity of anionic wormlike micelles: effects of ionic strength and small hydrophobic molecules, Soft Matter 9 (2013) 1203–1213.
[6] M. Pleines, W. Kunz, T. Zemb, D. Benczedi, W. Fieber, Molecular factors governing the viscosity peak of giant micelles in the presence of salt and fragrances, J. Colloid Interface Sci. 537 (2019) 682–693.
[7] Z. Mitrinova, H. Alexandrov, N. Denkov, S. Tcholakova, Effect of Counter-ion on Rheological Properties of Mixed Surfactant Solutions, Colloids Surf. A Physicochem. Eng. Asp. 643 (2022) 128746.
[8] Zhenghua Sun, Yahui Ji, Haicheng Wang, Jingyi Zhang, Cheng Yuan, Mingjie Kang, Yujun Feng, Hongyao Yi, Colloids Surf. A Physicochem. Eng. Asp. 700 (2024) 134831.
[9] Lorenzo Veronico, Luigi Gentile, Salt-Induced Modulation of Self-Assembly in C8-10 AlkylPolyGlucoside/Fatty Alcohol Formulations, ChemPlusChem 90 (2025) e202500390.
[10] Ewelina Warmbier-Wytykowska, Ashley P. Williams, Viviane Lutz-Bueno, Stephan Handschin, Sylwia Rozanska, Patrycja Wagner, Peter Fischer, Jacek Rozanski, Viscoelastic solutions of polyoxyethylene lauryl ethers and anionic surfactant mixtures: Headgroup and salt effects, J. Mol. Liq. 437 (2025) 128654.
[11] Ewelina Warmbier-Wytykowska, Milad Radiom, Patrycja Wagner, Sylwia Rozanska, Peter Fischer, Jacek Rozanski, J. Mol. Liq. 456 (2026) 129655.
[12] Z. Mitrinova, S. Tcholakova, N. Denkov, Control of Surfactant Solution Rheology Using Medium-Chain Cosurfactants, Colloids Surf. A Physicochem. Eng. Asp. 537 (2018) 173–184.
[13] W. Fieber, A. Scheklaukov, W. Kunz, M. Pleines, D. Benczédi, T. Zemb, Towards a general understanding of the effects of hydrophobic additives on the viscosity of surfactant solutions, J. Mol. Liq. 329 (2021) 115523.
[14] K. Aramaki, S. Hoshida, S. Arima, Effect of carbon chain length of cosurfactant on the rheological properties of nonionic wormlike micellar solutions formed by a sugar surfactant and monohydroxy alcohols, Colloids Surf. A 366 (2010) 58–62.
[15] M. Kamada, S. Shimizu, K. Aramaki, Manipulation of the viscosity behavior of wormlike micellar gels by changing the molecular structure of added perfumes, Colloids Surf. A Physicochem. Eng. Asp. 458 (2014) 110–116.
[16] Y. Fan, H. Tang, R. Strand, Y. Wang, Modulation of partition and localization of perfume molecules in sodium dodecyl sulfate micelles, Soft Matter 12 (1) (2016) 219–227.
[17] E. Fischer, W. Fieber, C. Navarro, H. Sommer, D. Benczédi, M.I. Velazco, M. Schönhoff, Partitioning and Localization of Fragrances in Surfactant Mixed Micelles, Surfact Deterg. 12 (2009) 73–84.
[18] X. Tang, W. Zou, P.H. Koenig, S.D. McConaughy, M.R. Weaver, D.M. Eike, M. J. Schmidt, R.G. Larson, Multiscale Modeling of the Effects of Salt and Perfume Raw Materials on the Rheological Properties of Commercial Threadlike Micellar Solutions, J. Phys. Chem. B 121 (2017) 2468–2485.
[19] T.M. McCoy, J.P. King, J.E. Moore, V.T. Kelleppan, A.V. Sokolova, L. Campo, M. de Manohar, T.A. Darwish, R.F. Tabor, The effects of small molecule organic additives on the self-assembly and rheology of betaine wormlike micellar fluids, J. Colloid Interface Sci. 534 (2019) 518–532.
[20] S. Isabettini, L.J. Böni, M. Baumgartner, K. Saito, S. Kuster, P. Fischer, V. Lutz-Bueno, Higher Salt Hydrophobicity Lengthens Ionic Wormlike Micelles and Stabilizes Them upon Heating, Langmuir 37 (2021) 132–138.
[21] V. Lutz-Bueno, S. Isabettini, F. Walker, S. Kuster, M. Liebi, P. Fischer, Ionic micelles and aromatic additives: A closer look at the molecular packing parameter, Phys. Chem. Chem. Phys. 19 (32) (2017) 21869–21877.
[22] M. Mirzamani, R.C. Reeder, C. Jarus, V. Aswal, B. Hammouda, R.L. Jones, E. D. Smith, H. Kumari, Effects of a Multicomponent Perfume Accord and Dilution on

the Formation of ST2S/CAPB Mixed-Surfactant Microemulsions, Langmuir 38 (2022) 1334–1347.
[23] I. Grillo, I. Morfin, S. Prévost, Structural characterization of pluronic micelles swollen with perfume molecules, LangmuiR 34 (2018) 13395–13408.
[24] C. Sofroniou, M. Baglioni, M. Mamusa, C. Resta, J. Doutch, J. Smets, P. Baglioni, Self-Assembly of Soluplus in Aqueous Solutions: Characterization and Prospectives on Perfume Encapsulation, ACS Appl. Mater. Interfaces 14 (2022) 14791–14804.
[25] Z. Mitrinova, Z. Valkova, S. Tcholakova, Interplay between cosurfactants and electrolytes for worm-like micelles formation, Colloids Surf. A 707 (2025) 135943.
[26] R. Ganguly, S. Kumar, A. Tripathi, M. Basu, G. Verma, H.D. Sarma, D.P. Chaudhari, V.K. Aswal, J.S. Melo, Structural and therapeutic properties of Pluronic® P123/F127 micellar systems and their modulation by salt and essential oil, J. Mol. Liq. 310 (2020) 113231.
[27] R. Ganguly, S. Kumar, M. Basu, A. Kunwar, D. Dutta, V.K. Aswal, Micellar solubilization of Lavender oil in aqueous P85/P123 systems: Investigating the associated micellar structural transitions, therapeutic properties and existence of double cloud points, J. Mol. Liq. 338 (2021) 116643.
[28] T.M. McCoy, A. Valiakhmetova, M.J. Pottage, C.J. Garvey, de, L. Campo, C. Rehm, D.A. Kuryashov, R.F. Tabor, Structural evolution of wormlike micellar fluids formed by erucyl amidopropyl betaine with oil, salts and surfactants, Langmuir 32 (47) (2016) 12423–12433.
[29] M. Mirzamani, A. Dawn, V.K. Aswal, R.L. Jones, E.D. Smith, H. Kumari, Investigating the effect of a simplified perfume accord and dilution on the formation of mixed surfactant microemulsions, RSC Adv. 11 (2021) 25858.
[30] M. Mirzamani, M. Flickinger, A. Dawn, V. Aswal, B. Hammouda, R.L. Jones, E. D. Smith, H. Kumari, Structural alterations of branched versus linear mixed-surfactant micellar systems with the addition of a complex perfume mixture and dipropylene glycol as cosolvent, RSC Adv. 12 (2022) 14998–15007.
[31] S.E. Anachkov, G.S. Georgieva, L. Abezgauz, D. Danino, P.A. Kralchevsky, Viscosity Peak due to Shape Transition from Wormlike to Disklike Micelles: Effect of Dodecanoic Acid, Langmuir 34 (2018) 4897–4907.
[32] ⟨https://hpvchemicals.oecd.org/UI/handler.axd?id=A05FF9F5-19B0-47F7-B40E-68EC10849BC7⟩.
[33] ⟨https://sitem.herts.ac.uk/aeru/ppdb/en/Reports/2013.htm⟩.
[34] ⟨https://www.acs.org/molecule-of-the-week/archive/l/limonene.html⟩.
[35] M.A.R. Martins, L.P. Silva, O. Ferreira, B. Schröder, J.A.P. Coutinho, S.M. Pinho, Terpenes solubility in water and their environmental distribution, J. Mol. Liq. 241 (2017) 996–1002.
[36] ⟨https://www.kremer-pigmente.com/elements/resources/products/files/87108e.pdf⟩⟨⟩.
[37] ⟨https://pubchem.ncbi.nlm.nih.gov/compound/Carvacrol#section=Solubility⟩.
[38] [⟨https://sitem.herts.ac.uk/aeru/bpdb/Reports/2012.htm⟩];
[39] B.D. Gute, S.C. Basak, D. Mills, D.M. Hawkins, Tailored Similarity Spaces for the Prediction of Physicochemical Properties, Internet Electron. J. Mol. Des. 1 (8) (2002) 374–387.
[40] S. Griffin, S.G. Wyllie, J. Markham, Determination of octanol–water partition coefficient for terpenoids using reversed-phase high-performance liquid chromatography, J. Chromatogr. A 864 (1999) 221–228.
[41] R.P. Souza, A.C. dos Reis, V.D. Pimente, B. Leal, S. de, M.M. de Freitas, J. Esteves, C. da, L.P.F. Ferreira, D.,C. Rodrigues, N. do, R.W.R. de Sousa, A.P. Lopes, M.J. dos Santos Soares, J.M. de Castro e Sousa, P.M.P. Ferreira, A.P. de Oliveira, Toxicogenetic profile and antioxidant evaluation of gamma-terpinene: Molecular docking and in vitro and in vivo assays, Drug. Chem. Toxicol. 48 (5) (2025).
[42] R.P. Souza, V.D. Pimentel, R.W.R. de Sousa, E.P. Sena, A.C.A. da Silva, D. Dittz, P. M.P. Ferreira, A.P. de Oliveira, Non-clinical investigations about cytotoxic and anti-platelet activities of gamma-terpinene, Naunyn Schmiede Arch. Pharmacol. 397 (10) (2024) 8145–8160.
[43] J. Li, E.M. Perdue, S.G. Pavlostathis, R. Araujo, Physicochemical properties of selected monoterpenes, Environ. Int. 24 (3) (1998) 353–358.
[44] S. Nikfar, A.F. Behboudi, Encyclopedia of Toxicology 3rd Edition, Editor: Philip Wexler, 2014.
[45] D. Prasanthi, P.K. Lakshmi, Terpenes: Effect of lipophilicity in enhancing transdermal delivery of alfuzosin hydrochloride, J. Adv. Pharm. Technol. Res. (4) (2012) 216–223.
[46] S. Banerjee, S.H. Yalkowsky, C. Valvani, Water solubility and octanol/water partition coefficients of organics. Limitations of the solubility-partition coefficient correlation, Environ. Sci. & Technol. 14 (10) (1980) 1227–1229.
[47] J. Sangster, Octanol-Water Partition Coefficients of Simple Organic Compounds, J. Phys. Chem. Ref. Data 18 (1989) 1111–1229.
[48] S.M. Vilas-Boas, M.C. da Costa, J.A.P. Coutinho, O. Ferreira, S.P. Pinho, Octanol–Water Partition Coefficients and Aqueous Solubility Data of Monoterpenoids: Experimental, Modeling, and Environmental Distribution, Ind. Eng. Chem. Res. 61 (8) (2022) 3154–3167.
[49] C. Hansch, S.M. Anderson, The effect of intramolecular hydrophobic bonding on partition coefficients, J. Org. Chem. 32 (8) (1967) 2583–2586.
[50] N.El Tayar, H. Waterbeemd, van de, M. Gryllaki, B. Testa, W.F. Trager, The lipophilicity of deuterium atoms. A comparison of shake-flask and HPLC methods, Int. J. Pharm. 19 (3) (1984) 271–281.
[51] M.M. Miller, S.P. Wasik, G.,L. Huang, W.,Y. Shiu, D. Mackay, Relationships between octanol-water partition coefficient and aqueous solubility, Environ. Sci. & Technol. 19 (6) (1985) 522–529.
[52] Y.B. Tewari, M.M. Miller, S.P. Wasik, D.E. Martire, Aqueous solubility and octanol/water partition coefficient of organic compounds at 25, 0 °C J. Chem. & Eng. Data 27 (4) (1982) 451–454.
[53] Y.-P. Chin, W.J. Weber Jr, T.C. Voice, Determination of partition coefficients and aqueous solubilities by reverse phase chromatography—II: evaluation of partitioning and solubility models, Water Res. 20 (11) (1986) 1443–1450.
[54] G.N. Reiner, D.O. Labuckas, D.A. Garcia, Lipophilicity of some GABAergic phenols and related compounds determined by HPLC and partition coefficients in different systems, J. Pharm. Biomed. Anal. 49 (3) (2009) 686–691.
[55] A. Turina, V. del, M.V. Nolan, J.A. Zygadlo, M.A. Perillo, Natural terpenes: Self-assembly and membrane partitioning, Biophys. Chem. 122 (2006) 101–113.
[56] C. Hansch, A. Leo, Exploring QSAR: Fundamentals and Applications in Chemistry and Biology, American Chemical Society, Washington DC, 1995.
[57] Q. Zhang, J.E. Grice, P. Li, O.G. Jepps, G.-J. Wang, M.S. Roberts, Skin Solubility Determines Maximum Transepidermal Flux for Similar Size Molecules, Pharm. Res. 26 (8) (2009) 1974–1985.
[58] P. Prerna, J. Chadha, L. Khullar, U. Mudgil, K. Harjai, A Comprehensive Review on the Pharmacological Prospects of Terpinen-4-Ol: From Nature to Medicine and Beyond, Fitoterapia 176 (2024) 106051.
[59] G.L. Biagi, O. Gandolfi, M.C. Guerra, A.M. Barbaro, G. Cantelli-Forti, Rm values of phenols. Their relation with log P values and activity, J. Med. Chem. 18 (9) (1975) 868–873.
[60] M. Thakur, A. Agarwal, A. Thakur, P.V. Khadikar, QSAR study on phenolic activity: need of positive hydrophobic term (logP) in QSAR, Bioorg. & Med. Chem. 12 (2004) 2287–2293.
[61] J. Saarikoski, M. Viluksela, Relation between physicochemical properties of phenols and their toxicity and accumulation in fish, Ecotoxicol. Environ. Saf. 6 (6) (1982) 501–512.
[62] M.E. Cates, S.J. Candau, Statics and dynamics of worm-like surfactant micelles, J. Phys. Condens. Matter 2 (1990) 6869–6892.
[63] H. Rehage, H. Hoffmann, Rheological properties of viscoelastic surfactant systems, J. Phys. Chem. 92 (1988) 4712–4719.
[64] H. Rehage, H. Hoffmann, Viscoelastic surfactant solutions: Model systems for rheological research, Mol. Phys. 74 (1991) 933–973.
[65] M.S. Turner, M.E. Cates, Linear viscoelasticity of living polymers: A quantitative probe of chemical relaxation times, Langmuir 7 (1991) 1590–1594.
[66] F. Kern, P. Lemarechal, S.J. Candau, M.E. Cates, Rheological properties of semidilute and concentrated solutions of cetyltrimethylammonium bromide in the presence of potassium bromide, Langmuir 8 (1992) 437–440.
[67] S. Zeppieri, J. Rodríguez, López, A.L. de Ramos, Interfacial Tension of Alkane + Water Systems, J. Chem. Eng. Data 46 (2001) 1086–1088.
[68] L. Svarovsky, Characterization of particles suspended in liquids. Solid-Liquid Separation, Butterworths, London, 1981. Chapter 2.
[69] C. Orr, Emulsion droplet size data. Encyclopedia of Emulsion Technology, Marcel Dekker, New York, 1983. Chapter 6.
[70] J.F. Ontiverosa, F. Boutona, M. Duranda, C. Pierlota, C. Quellet, V. Nardello-Rataja, J.-M. Aubry, Dramatic influence of fragrance alcohols and phenols on the phaseinversion temperature of the Brij30/n-octane/water system, Colloids Surf. A Physicochem. Eng. Asp. 478 (2015) 54–61.
[71] N. Kanei, Y. Tamura, H. Kunieda, Effect of Types of Perfume Compounds on the Hydrophile–Lipophile Balance Temperature, J. Colloid Interface Sci. 218 (1999) 13–22.